ARPA Order No. 1479

Contract No. N00014-67-A-0216-0023

Program Code 1E20

Principal Investigator: W. R. Brennen

Address: Department of Chemistry
University of Pennsylvania
215 S. 34 Street
Philadelphia, Pennsylvania 19104

Phone: (215) 594-8622

Name of Contractor:

University of Pennsylvania
Philadelphia, Pennsylvania 19104

Short Title of Work:

Excitation of Nickel by Active Nitrogen

Effective Date of Contract:

From October 1, 1970 To September 30, 1971

Amount of Contract: $35,000.

Sponsored by

Advanced Research Projects Agency

ARPA Order 1479

Security Classification

DOCUMENT CONTROL DATA - R&D

(Security classification of title, body of abstract and indexing annotation must be entered when the overall report is classified)

1. ORIGINATING ACTIVITY (Corporate author)

University of Pennsylvania
Philadelphia, Pennsylvania 19104

2a. REPORT SECURITY CLASSIFICATION

Unclassified

2b. GROUP

3. REPORT TITLE

EXCITATION OF ATOMIC NICKEL IN THE REACTION BETWEEN NICKEL CARBONYL AND ACTIVE NITROGEN.

4. DESCRIPTIVE NOTES (Type of report and inclusive dates)

Final Technical Report

5. AUTHOR(S) (Last name, first name, initial)

Shane, Edward C. and Brennen, William R.

6. REPORT DATE	**7a. TOTAL NO. OF PAGES**	**7b. NO. OF REFS**
August 28, 1972	49	24

8a. CONTRACT OR GRANT NO.	**9a. ORIGINATOR'S REPORT NUMBER(S)**
N00014-67-A-0216-0023	
b. PROJECT NO. NR 012-211	
c.	**9b. OTHER REPORT NO(S) (Any other numbers that may be assigned this report)**
d.	

10. AVAILABILITY/LIMITATION NOTICES

Distribution of this document is unlimited.

11. SUPPLEMENTARY NOTES	**12. SPONSORING MILITARY ACTIVITY**
	Advanced Research Projects Agency (STO)

13. ABSTRACT

The emission spectrum of the active nitrogen-nickel carbonyl reaction flame between 2300A and 7600A has been measured in a discharge/flow system at pressures between 0.13 and 27 torr. Relative populations and relative rates of formation of excited states of atomic nickel have been calculated, and various effects of reaction conditions and gas composition have been investigated. To the extent testable, the results are consistent with a mechanism in which atomic nickel produced in the reaction is excited by collision with metastable $N_2(A^3\Sigma_u^+)$ molecules in various vibrational levels produced in active nitrogen. The pressure dependence of the atomic nickel spectrum results mainly from changes in the vibrational distribution of the $N_2(A)$ molecules.

I

DD FORM 1 JAN 64 1473

Security Classification

KEY WORDS	LINK A		LINK B		LINK C	
	ROLE	WT	ROLE	WT	ROLE	WT
Atomic nickel excitation						
Active nitrogen reaction						
Quantitative emission spectroscopy						
Nickel carbonyl						

INSTRUCTIONS

1. ORIGINATING ACTIVITY: Enter the name and address of the contractor, subcontractor, grantee, Department of Defense activity or other organization *(corporate author)* issuing the report.

2a. REPORT SECURITY CLASSIFICATION: Enter the overall security classification of the report. Indicate whether "Restricted Data" is included. Marking is to be in accordance with appropriate security regulations.

2b. GROUP: Automatic downgrading is specified in DoD Directive 5200.10 and Armed Forces Industrial Manual. Enter the group number. Also, when applicable, show that optional markings have been used for Group 3 and Group 4 as authorized.

3. REPORT TITLE: Enter the complete report title in all capital letters. Titles in all cases should be unclassified. If a meaningful title cannot be selected without classification, show title classification in all capitals in parenthesis immediately following the title.

4. DESCRIPTIVE NOTES: If appropriate, enter the type of report, e.g., interim, progress, summary, annual, or final. Give the inclusive dates when a specific reporting period is covered.

5. AUTHOR(S): Enter the name(s) of author(s) as shown on or in the report. Enter last name, first name, middle initial. If military, show rank and branch of service. The name of the principal author is an absolute minimum requirement.

6. REPORT DATE: Enter the date of the report as day, month, year; or month, year. If more than one date appears on the report, use date of publication.

7a. TOTAL NUMBER OF PAGES: The total page count should follow normal pagination procedures, i.e., enter the number of pages containing information.

7b. NUMBER OF REFERENCES: Enter the total number of references cited in the report.

8a. CONTRACT OR GRANT NUMBER: If appropriate, enter the applicable number of the contract or grant under which the report was written.

8b, 8c, & 8d. PROJECT NUMBER: Enter the appropriate military department identification, such as project number, subproject number, system numbers, task number, etc.

9a. ORIGINATOR'S REPORT NUMBER(S): Enter the official report number by which the document will be identified and controlled by the originating activity. This number must be unique to this report.

9b. OTHER REPORT NUMBER(S): If the report has been assigned any other report numbers *(either by the originator or by the sponsor)*, also enter this number(s).

10. AVAILABILITY/LIMITATION NOTICES: Enter any limitations on further dissemination of the report, other than those imposed by security classification, using standard statements such as:

(1) "Qualified requesters may obtain copies of this report from DDC."

(2) "Foreign announcement and dissemination of this report by DDC is not authorized."

(3) "U. S. Government agencies may obtain copies of this report directly from DDC. Other qualified DDC users shall request through

_____."

(4) "U. S. military agencies may obtain copies of this report directly from DDC. Other qualified users shall request through

_____."

(5) "All distribution of this report is controlled. Qualified DDC users shall request through

_____."

If the report has been furnished to the Office of Technical Services, Department of Commerce, for sale to the public, indicate this fact and enter the price, if known.

11. SUPPLEMENTARY NOTES: Use for additional explanatory notes.

12. SPONSORING MILITARY ACTIVITY: Enter the name of the departmental project office or laboratory sponsoring *(paying for)* the research and development. Include address.

13. ABSTRACT: Enter an abstract giving a brief and factual summary of the document indicative of the report, even though it may also appear elsewhere in the body of the technical report. If additional space is required, a continuation sheet shall be attached.

It is highly desirable that the abstract of classified reports be unclassified. Each paragraph of the abstract shall end with an indication of the military security classification of the information in the paragraph, represented as *(TS)*, *(S)*, *(C)*, or *(U)*.

There is no limitation on the length of the abstract. However, the suggested length is from 150 to 225 words.

14. KEY WORDS: Key words are technically meaningful terms or short phrases that characterize a report and may be used as index entries for cataloging the report. Key words must be selected so that no security classification is required. Identifiers, such as equipment model designation, trade name, military project code name, geographic location, may be used as key words but will be followed by an indication of technical context. The assignment of links, roles, and weights is optional.

II

DD FORM 1 JAN 64 1473 (BACK)

Final Technical Report

EXCITATION OF ATOMIC NICKEL IN THE REACTION BETWEEN NICKEL CARBONYL AND ACTIVE NITROGEN

by

E. C. Shane and W. R. Brennen

Department of Chemistry

University of Pennsylvania

Philadelphia, Pennsylvania 19104

ONR Contract N00014-67-A-0216-0023

NR 012-211

ARPA Order No. 1479

III

INTRODUCTION

Since the observation of Strutt[1] that the line spectra of various metals are developed when the metals are exposed to active nitrogen, several studies[2,3,4,5] of excitation of metal atoms in active nitrogen have been made. Brennen and Kistiakowsky[5] found that $Ni(CO)_4$, $Fe(CO)_5$, $Cr(CO)_6$, $W(CO)_6$, $Mn_2(CO)_{10}$, and $Co(NO)(CO)_3$ reacted rapidly with active nitrogen, forming metal atoms, and producing flames due to metal atom emission spectra. We have looked in greater detail at the $Ni(CO)_4$-active nitrogen reaction. Emission spectra were observed between 0.13 and 27 torr and found to be pressure dependent. A simple excitation mechanism is presented and the effect of quenching and the applicability of the Franck-Concon principle to the energy transfer reaction are discussed. The effect of reactant ratio, observation time, and added gases on the atomic flame are evaluated.

EXPERIMENTAL SECTION

The $Ni(CO)_4$-active nitrogen reaction was studied in a 25mm o.d. pyrex flow tube fitted with a fused silica observation window mounted parallel to the axis of the flow tube as shown in Fig. (1). Gas inlet jets were located immediately before the observation window and 19 cm upstream. For one experiment an inlet jet was located 5.3 cm upstream from the observation instead of right at it. Downstream from the flow tube were a 15 mm bore, right angle throttling stopcock, two U-traps, one of which was detachable, a 10 mm bore right angle stopcock, a 2-liter ballast bulb, and a mechanical pump. While $Ni(CO)_4$ was flowing both U-traps were maintained at liquid nitrogen temperature. Light emitted by the reaction flame passed through the fused silica window and was directed by two reflecting mirrors into a 3/4 meter

Czerny-Turner, Jarrell-Ash scanning monochromator located about 34 cm distant. For wavelengths between 4000 and 7600A a Corning 3060 filter was inserted just before the entrance slit of the monochromator. Primarily photoelectric measurements were made using a dry ice-cooled EMI-9558 photomultiplier tube with magnetic defocusing operated at 860V from a Northeast Model RE-1602 stabilized high-voltage power supply. The output of the photomultiplier tube was amplified by a Keithley Model 610-BR electrometer and displayed on a Leeds and Northrup Speedomax-G strip chart recorder. Typical monochromator slit widths were 152-200μ giving a band pass of about 1.5 to 2.0A. A few photographic measurements were made using 50 μ slits and Kodak 103-F photographic plates.

The relative sensitivity between 2500 and 7500Å of the 0.75 m monochromator and EMI-9558QA photomultiplier tube was calibrated with a standard tungsten-iodine lamp from the Eppley Corporation. Over a one-year period no change in the relative sensitivity was detected. A plot of the sensitivity, defined as the photomultiplier tube output in amps at a given wavelength devided by the standard lamp output in quanta/sec, against wavelength is given in Fig. (3). A correction for a slight change in reciprocal linear dispersion over the wavelength range is included.

Nitrogen atoms were formed in either an electrodeless, microwave discharge in a fused silica tube located 70 cm upstream from the flow tube or a pulsed discharge tube located 140 cm upstream. The microwave discharge was powered by a 2450 MHz, 100 W Raytheon Model PGM-10 microwave power generator coupled to a Type 5^6, 1/4 wave cavity supplied by Ophthos Instruments. The pulsed discharge was maintained in a water-cooled, pyrex discharge tube, Fig. (2a), fitted with two stainless steel hollow electrodes. The condensed discharge circuit, Fig. (2b), employed a Sorenson High Voltage Supply Model 1006-100

with a maximum output of 6000V and 100mA. The power supply charged a Tobe Deutschmann 1 μF, 10,000V capacitor. The rate of firing was regulated by a spark gap with two opposing brass rods with hemispherical ends separated by a rotating brass conductor. The entire spark gap assembly was enclosed in a plexiglass box which was flushed with nitrogen. The rate of rotation of the center conductor was regulated by a series motor powered by a Variac. The rpm of the motor and thus the pulse rate was easily regulated with the Variac. Typically the pulsed discharge was run at 5000V with a pulse rate of 8-15 pulses/sec. After several hours of running the nitrogen atom concentration began to fall. Apparently metal which sputtered from the electrodes deposited on the exit tube where it enhanced wall recombination of the nitrogen atoms. Rinsing with a 10% aqueous HF solution removed any deposited metal.

The nitrogen atom concentration was determined by NO titration using a visual endpoint. The flow rate of NO, $Ni(CO)_4$, and added gases such as CO and C_2H_2 were measured by timing a pressure drop in a calibrated volume[7] using Dow-Corning DC-704 silicone oil (ρ=1.063 g/cc at 25°C) as the working fluid in the differential manometer. The nitrogen diluent flowrate was measured using a Poiseuille flowmeter described previously.[8]

The diluent nitrogen was either prepurified nitrogen obtained from the Matheson Company or white spot nitrogen from the Air Products Company. Technical grade (98.5%) NO, $Ni(CO)_4$, and C_2H_2 (99.6%) were obtained from the Matheson Company. CO (99.3%) was obtained from the Air Products Company. NO was purified by vacuum distillation from a trap maintained at 113°K to one cooled with liquid nitrogen, with initial and final fractions being discarded. The $Ni(CO)_4$ was purified by freezing down in a liquid nitrogen trap and pumping with a mechanical pump and then a Hg diffusion pump. The liquid nitrogen was then removed and the $Ni(CO)_4$ was distilled to a trap at -77°C

with initial and final fractions being discarded. The $Ni(CO)_4$ was a colorless liquid at room temperature. C_2H_2 was purified by vacuum distillation from a trap maintained at 196°K to one cooled with liquid nitrogen. CO was passed through a glass wool-packed U-trap at 78°K and was added directly to a storage bulb. Gases were always conducted from the tanks in glass tubing. Glass-metal connections were all made either with soldered Kovar seals or with epoxy adhesive.

As the $Ni(CO)_4$-active nitrogen reaction proceeded a black deposit occurred on the downstream walls of the flowtube and on the mouth of the $Ni(CO)_4$ inlet. Coating the walls of the flowtube with 85% phosphoric acid saturated with phosphorus pentoxide allowed at least 5 hours of operation before buildup of the deposit on the walls became objectionable.

All measurements were taken at room temperature, which averaged 22 ± 3°C.

RESULTS

Description of the Flame

The addition of $Ni(CO)_4$ to a flow of discharged nitrogen produced a conical, bright blue flame which extended down the flow tube. The brightest flames were obtained for runs around 3 torr. For $[Ni(CO)_4]$ on the order of $[N]$ the flame was typically observed for at least 15 cm downstream. Under these conditions the yellow afterflow was also visible downstream of the carbonyl inlet. Increasing the flow of the $Ni(CO)_4$ increased the width of the conical flame, decreased the extent to which it extended downstream, and decreased the intensity of the yellow afterglow downstream. As the pressure was decreased to 0.3 and 0.13 torr the blue flame became very diffuse. At 0.14 torr the flame extended about 3 cm upstream and 10-15 cm downstream. At these low pressures

it was necessary to increase the length of the sidearm to which the fused silica window was attached. Otherwise, the flame extended out to the window and a black deposit eventually coated the window so extensively the observed intensity was drastically reduced although the flame was approximately constant. As the pressure in the flow tube was increased to 9.6, 14.7, and 27 torr the flame began to develop what appeared to be a reddish cone inside the blue cone.

On occasion, especially with added O_2, when the $Ni(CO)_4$ was shut off and only the yellow nitrogen afterglow was present, a distinct red glow was present on the walls of the flow tube where the black deposit was present. This was assumed to be the surface catalyzed excitation of nitrogen that has been studied by Harteck, Mannella, and Reeves.[9] Since there is also a (nickel) deposit at the carbonyl inlet, it is possible that the reddish inner cone observed at higher pressures may be due to this phenomenon.

Pressure Dependence of the Atomic Nickel Emission Spectra

The atomic nitrogen-nickel carbonyl flame consists almost entirely of emission from excited nickel atoms. The only other emission observed was weak CN violet emission. No other emission has been detected in the wavelength range from 2300 to 7600A. Table I lists most of the stronger lines, the energy level of the emitting state and its term symbol, and the relative intensities of the lines at a representative number of pressures between 0.13 and 27 torr. The type of discharge, pulsed (P) or microwave (M), is indicated in the parentheses next to the pressure. The data for 0.13 and 0.54 torr had 0.6% O_2 added before the discharge to promote dissociation on the nitrogen. All intensities are recorded relative to an arbitrarily chosen standard peak at 3369.57A which has been assigned an intensity of 500. Over the several hours necessary for one run the flame intensity was often found to decrease

by about 15-30% due to clogging of the carbonyl inlet with a solid deposit. In all runs the standard peak was swept repeatedly, any changes in flame intensity were assumed to be linear, and the observed relative intensities were adjusted to standard conditions by linear interpolation. Results at a given pressure are considered reproducible to within 10-15%.

Experiments were run using a microwave discharge for runs greater than 1 torr and a pulsed discharge for runs less than 1 torr. Data taken with both the pulsed discharge and the microwave discharge at 1.0 torr gave identical results within scatter.

Wavelength assignments were made by comparing the photoelectric spectra with the compilation of atomic nickel lines by Corliss.[10] Line identifications were verified between 2300 and 5200A by photographic spectra taken with 50 μ slits (0.5A bandpass) and analyzed on a measuring microscope.

Reactant Ratio

The nitrogen atom and $Ni(CO)_4$ concentrations used in the reported data are summarized in Table II. One experiment was performed to determine if the reactant ratio affected the observed relative intensities. At 1.8 torr five runs were taken in which the reactant ratio, $[N]/[Ni(CO)_4]$, was varied between 4.5 and 29 and representative strong lines over the entire wavelength range were recorded. Within normal fluctuation the relative intensities were not affected by changing reactant ratio.

Observation Time

The linear flowrate of the diluent nitrogen varied for the different pressure runs between about 100 cm/sec and 550 cm/sec. The higher pressure runs had lower flowrates due to throttling and the lower pressure runs had lower flowrates due to decreased pumping efficiency. Since the carbonyl inlet was stationary, slightly different portions of the atomic flame were observed.

Two experiments were performed to determine if the observation time after mixing had any affect on the observed relative intensities. At 1.8 torr two runs were taken with linear flowrates of 100 and 550 cm/sec. The relative intensities were the same for the two runs. For all runs mentioned thus far the $Ni(CO)_4$ was added through the inlet at the observation window. Two runs were performed in which $Ni(CO)_4$ was added through the upstream inlets. With the $Ni(CO)_4$ added through the inlet 19 cm upstream at a total pressure of 3.6 torr the observed intensities were very weak, and thus not well determined, but within the accuracy of the data the relative intensities were not affected by the inlet position. At 9.5 torr $Ni(CO)_4$ was added through the inlet 5.3 cm upstream (equivalent to 4×10^{-2} sec at the prevailing flowrate) and compared to the run with $Ni(CO)_4$ added at the observation window. Within scatter there was no change in the relative intensities. The observed relative intensities are not affected by changes in observation time to the extent which they are varied in these experiments.

Effect of Added Gases on Relative Intensities

a) Oxygen added before the discharge

Oxygen when added to the nitrogen flow before the pulsed discharge has no appreciable affect on the relative intensities. The addition of 0.6% O_2 to a run with the pulsed discharge at 0.3 torr gave relative intensities about 20% lower than a run without added O_2. Thus the 0.13 torr run with 0.6% O_2 recorded in Table I is not significantly affected by the added O_2.

With O_2 added before the microwave discharge there was an effect, though small. A run at 1.85 torr with 0.3% O_2 had all peaks increased by an average of about 20% relative to the standard peak. For a run at 1.1 torr with 0.6% added O_2 lines with $E_u > 40{,}000$ cm^{-1} increased about 15%. A comparison for lower pressures can be made using the data in Table I. It was

not possible to perform low pressure experiments with a microwave discharge and no added O_2 because of the forbiddingly low nitrogen atom concentration and consequent weak atomic flame. However, the pulsed discharge experiment at 0.3 torr can be compared with the microwave discharge experiments at 0.4 torr with 0.6% O_2. In both cases two runs giving very similar results were averaged to give the reported data so the accuracy is fairly good. Again the microwave discharge with added O_2 gives higher relative intensities for lines with $E_u > 40{,}000\ cm^{-1}$. For lines with $E_u < 40{,}000\ cm^{-1}$ the increase in relative intensity with added O_2 is only slightly greater than normal scatter. However, lines originating from the higher energy states had increases in relative intensity that were larger than reasonable scatter. It does appear that these higher energy states are increased in intensity relative to the lower states. A possible explanation is that the lower states or their precursor are quenched by O_2 or a discharge product of O_2. Since the effect is not observed with a pulsed discharge it would appear that a microwave discharge product of O_2 is involved. Considering, however, the marginal extent of the observed effect, very little can be said in this matter.

b) Added C_2H_2

For a run at 1.8 torr with a partial pressure of added $Ni(CO)_4$ of 0.9×10^{-3} torr, C_2H_2 was added in four differing amounts between 0.9×10^{-3} torr and 1.2×10^{-2} torr. There was no effect on the relative intensities of a representative sampling of lines. For a run at 5.6 torr 4×10^{-3} torr of C_2H_2 had no effect on a flame with 1.7×10^{-3} torr added $Ni(CO)_4$.

c) Added CO

The addition of CO to the carbonyl flame at 2.1 torr in concentrations between 3 to 20 times that of $Ni(CO)_4$ had no effect on the observed relative intensities.

Trap Analysis

The black deposits taken from the carbonyl inlet and from the U-traps downstream of the reactor were analyzed for nickel content using either a titration with sodium ethylenediaminetetraacetate (EDTA)[11] and muroxide indicator or precipitation with dimethylglyoxime (DMG)[11]. The results are summarized in Table III. The deposit in the inlet is almost entirely nickel metal. The deposit collected in the U-traps appears to vary in nickel content between 35-70%. The trap deposit may consist of nickel plus a polymeric compound or nickel as part of a polymeric compound. Frequently, sparks were observed in the U-traps when air was introduced, so apparently at least a portion of the deposit is some form of active nickel "black", which is pyrophoric.

CN Violet Band System

CN violet ($B^2\Sigma^+ \rightarrow X^2\Sigma^+$) emission has been observed weakly in the carbonyl flame at low pressures and with a moderate intensity in the high pressure flames. Some of the observed bands at several pressures are summarized in Table IV. The CN emission is present only when $Ni(CO)_4$ is added; it is not an impurity emission.

The study of CN emission in flames is a very complex matter with several different proposed mechanisms of CN excitation[12-17,4]. A reaction mechanism proposed for the active nitrogen-nickel carbonyl reaction by Brennen and Kistiakowsky[5] included CO as a reaction product and NCO as an intermediate. The reaction of atomic nitrogen with CO to form ground state CN is 74 kcal/mole endothermic and will not be important. The reaction, $N + NCO \rightarrow CN + NO$, is 7 kcal/mole exothermic and may provide a source of ground state CN. The CN could then be excited to its $B^2\Sigma$ state by collision with $N_2(A^3\Sigma_u^+)$, which is present in the active nitrogen. Such a mechanism has been proposed by

Bayes[12] and supported by Campbell and Thrush[15]. The similar CN vibrational level distribution found at 9.6, 14-7, and 27 torr suggests that just one mechanism is operating at these pressures.

DISCUSSION

Excitation of Metal Atoms by Active Nitrogen

Since the earliest observations of Strutt[1] that the line spectra of various metals - cadmium, magnesium, mercury, potassium, zinc, and lead - are developed when the metals are exposed to active nitrogen, several studies[2-5] of excitation of metal atoms in active nitrogen have been made. Brennen and Kistiakowsky[5] (BK) found that $Ni(CO)_4$, $Fe(CO)_5$, $Cr(CO)_6$ $W(CO)_6$, $Mn_2(CO)_{10}$, and $Co(NO)(CO)_3$ reacted rapidly with active nitrogen, forming metal atoms, and producing flames due to metal atom emission spectra. Studying the $Ni(CO)_4$ and $Fe(CO)_5$ reactions in detail BK concluded that a stepwise degradation occurred

$$\begin{aligned} M(CO)_n + N &\longrightarrow M(C))_{n-1} + NCO, \text{ etc.} \\ M(CO) + N &\longrightarrow M(g) + NCO \\ M(g) + \text{wall} &\longrightarrow M(s) \\ 2NCO &\longrightarrow N_2 + 2CO \\ N + NCO &\longrightarrow N_2 + CO \end{aligned} \qquad (1)$$

where M is the metal atom. The emission spectra was concluded to result from excitation of metal atoms in collision with metastable $N_2(A^3\Sigma_u^+)$ molecules. Phillips[2,3], observing primarily the thallous halides, concluded that the thallium atom was excited in a termolecular process.

$$Tl X + N + N \longrightarrow Tl^* + N_2 + X \qquad (2)$$

X = halogen

or in a bimolecular reaction of TlX with an excited nitrogen molecule formed

during N-atom recombination

$$\begin{aligned} N + N + N_2 &\longrightarrow N_2^* + N_2 \\ N_2^* + Tl X &\longrightarrow N_2 + Tl^* + X \end{aligned} \qquad (3)$$

Since the Tl atoms were assumed to be formed as the result of a dissociative collision process, it was necessary for N_2^* to have at least 225 kcal/mole of energy to form Tl in its observed states. $N_2(^5\Sigma)$ was considered to be the most probable excited nitrogen molecule. It is possible that the reaction of the thallous halides with active nitrogen also involves stripping of the halide atom in the reaction of TlX with a N-atom and consequent excitation of the free Tl-atom in collision with a $N_2(A)$ molecule. The observations led Phillips to discount a degradation mechanism: (1) no Tl emission was found in the region immediately following the flame, and (2) the addition of Tl vapor alone to active nitrogen resulted in a much weaker flame. If in either of these cases the Tl-atom concentration were significantly lower than in the TlX flame, a much weaker emission flame would be expected. The addition of Tl vapor, indeed, suggests that the Tl-atom can be directly excited by active nitrogen.

Our observations of the $Ni(CO)_4$ flame are similar to those of BK[5]. We found that the relative intensities of the various nickel lines is the same at the reaction inlet and at positions much further downstream. This supports the proposed degradation mechanism of BK with excitation of gaseous nickel atoms by $N_2(A)$ which is present in the active nitrogen downstream of the reaction flame. We have observed excited nickel atoms with up to about 57,000 cm^{-1} of energy above the ground state, in agreement with BK. Our observations were limited primarily to states with $E_u < 52{,}000$ cm^{-1}. If Ni is assumed to be excited from its ground state, then $N_2(A)$ molecules in vibrational levels up to at least $v' = 6$ are necessary to supply the required

excitation energy. Ni has low lying states which may be populated to some degree. An absorption study of the carbonyl flame is necessary to determine if the low lying states are appreciably populated. If they are, then slightly lower vibrational levels of $N_2(A)$ could supply the necessary excitation energy.

Pressure Dependence of the Relative Steady-State Population Distribution

Relative steady-state populations for the excited nickel levels were calculated from the relative intensities recorded in Table I. The relative intensities were corrected for the relative sensitivity of the photomultiplier tube and monochromator, Fig. (3), and populations were calculated from the relationship

$$N_u \propto \frac{g_u I \lambda^2}{g_\ell f_{\ell u}} \qquad (4)$$

where N_u is the steady-state population, I is the relative intensity in units of quanta, λ is the wavelength, $f_{\ell u}$ is the absorbtion oscillator strength, and g_u and g_ℓ are the degeneracies of the upper and lower states of a transition, respectively. g-Values were taken from Corliss[10]. Plots of relative population against energy of the upper state are given in Fig. (4) through Fig (11) for pressures between 0.13 and 27 torr. A line representing an effective Boltzmann temperature is drawn through the data. Considering the scatter in the data the temperature is accurate to about $\pm$ 400°K. A significant change in the relative population distribution is found over the pressure range studied as demonstrated by the change in effective temperature. A plot of the observed effective temperature against pressure is given in Fig. (12).

For purposes of qualative evaluation of trends the nickel population has been divided into four groups with different E_u: (1) group I, $28{,}000 < E_u < 31{,}000$ cm^{-1}; (2) group II, $31{,}000 < E_u < 37{,}000$ cm^{-1}; (3) group III, $42{,}000 < E_u < 45{,}000$ cm^{-1}; and (4) group IV, $45{,}000 < E_u < 52{,}000$ cm^{-1}. We have taken only limited data for energy levels above 52,000 cm^{-1}. Observation

of Fig. (4) through Fig. (11) reveals that in addition to the overall change in relative population there has been a noticeable change in the relative position of group II. The effective temperature line has been drawn largely through groups I, III, and IV. At lower pressures the group II points fall below this temperature line while at the higher pressures they have increased in population and fall very nicely in line. Between 0.13 and 27 torr group II has risen from an average of about 25% lower in population than group I to a population very nearly equal to group I.

With two exceptions the relative populations within a given group did not change with pressure. That is, the higher population points within group IV at 0.13 torr and 27 torr represent the same emission lines, etc. The 3371.99A and 2994.46A lines violate this trend and will be discussed below in the section on quenching.

The lower energy levels of Ni can be populated by radiative cascading from higher levels. Relative intensities for data at 9.6 torr were converted to intensities proportional to quanta/sec and the ratio of cascading from higher levels, E_u = 42-52,000 cm^{-1}, to radiative depletion was calculated. For levels with $26,000 < E_u < 32,000$ cm^{-1} the ratio was 0.13, and for levels with $32,000 < E_u < 37,000$ cm^{-1} the ratio was 0.16. An estimate was also made including lines listed in "Tables of Spectral-line Intensity" by Meggers, et al.[18] that we did not observe directly. The ratios were only minimally changed by this correction. It can be seen from the low ratios that the population of the lower levels is not affected appreciably by radiative cascading.

Excitation Mechanism

A mechanism which describes the excitation of the Ni-atoms is as follows:

$$N_2(A^3\Sigma,\ v=v') + Ni(g) \xrightarrow{k} Ni^* + N_2\ (X^1\Sigma,\ v=v'')$$

$$Ni^* \longrightarrow Ni + h\nu \qquad (5)$$

$$Ni^* + N_2 \xrightarrow{k_Q} \text{Quench}$$

Excited nickel atoms, Ni^*, are formed in collision with the metastable $N_2(A)$ molecule which drops to its ground state. The excited nickel atoms are depopulated by radiation or quenching by nitrogen buffer. The population distribution in Ni^* reflects the energy distribution in the vibrational levels of $N_2(A)$ and the rate of population of the different excited states of nickel. If the quenching step is neglected (discussion below of the quenching step suggests this is a reasonable assumption) the rate of formation of a given energy level, E_u, is represented as

$$R = N_u/\tau_u \qquad (6)$$

where N_u is the steady-state population and τ_u is the radiative lifetime. Using relative populations and calculated radiative lifetimes (see below, Table VI), relative rates of formation of some of the states with strong emission lines have been evaluated at 0.13, 2.4, and 27 torr. See Figs. (13) to (15).

An attempt was made to calculate an expected rate of formation of Ni^* as a function of E_u using a known vibrational distribution for $N_2(A)$. An important issue in this calculation is the importance of the Franck-Condon principle for the $N_2(A) \rightarrow N_2(X)$ transition in determining the energy that is available in a bimolecular collision with Ni(g). Robertson[19] in a study of collision of excited Ar atoms with molecules has concluded that the molecules do obey the Franck-Condon principle. Transitions in which molecular separations are maintained constant are the most favored. Callear and Wood[20] have considered the energy transfer reactions of $N_2(A)$ with a series of other molecules. They concluded that to the first approximation of $N_2(A) \rightarrow N_2(X)$ transition obeyed the Franck-Condon principle.

In a separate study[21] the $N_2(A)$ vibrational population distribution was determined under a variety of conditions. Table V is a summary of the observed relative vibrational populations at 2.4 and 40 torr. The relative rates of formation were calculated according to

$$\frac{d[Ni^* \text{ (group I)}]}{dt} \propto k(q_{v'v''}) [N_2(A, v=v')][Ni(g)] \tag{7}$$

for all transitions in the range E(A, v=v') - E(X, v=v'') = E (group I), etc. The rate of energy transfer from $N_2(A)$ to Ni(g) was considered to be of the form[19]

$$k = v [\sigma P_E(\Delta E)] q_{v'v''} \tag{8}$$

where v is the relative velocity of the collision partners, σ is the reaction cross section, $P_E(\Delta E)$ is the potential energy part of the cross section, and $q_{v'v''}$ is the Franck-Condon factor. For calculation of relative rates of formation the cross sections are all assumed to be equal so that

$$k \propto q_{v'v''} \tag{9}$$

Several $N_2(A)$ vibrational levels feed into a given energy range so the relative rates of formation were summed according to group. $[q_{v'v''}] [A_{v'}]$ was evaluated for various v''s and summed for all transitions with the energy for the $N_2(A) \rightarrow N_2(X)$ transition within the energy range for group I, etc. The F-C factors were taken from Benesch et al.[22]. The calculated relative rates of formation are shown as squares in Fig. (14) and Fig. (15). The relative rates are recorded at an average energy for a given group. There is good agreement between the calculated and observed relative rates of formation. The agreement indicates that to a first approximation the proposed mechanism adequately describes the excitation of nickel atoms. The assumption that the Franck-Condon principle applies for the $N_2(A) \rightarrow N_2(X)$ transition in collision

appears to be valid. Indeed, the nickel carbonyl-active nitrogen reaction provides a good test of the applicability of the Franck-Condon principle in bimolecular collisions. In the energy transfer reactions of $N_2(A)$ with other molecules[21] only a limited number of acceptor states are available. With the Ni-atom a whole manifold of acceptor states are available. It is desirable to look at the excitation of other metals, with reasonably extensive energy manifolds, by $N_2(A)$ to determine if the Franck-Condon principle is generally applicable in collisions. The reaction of other metal carbonyls with active nitrogen provides a very convenient method for studying this process.

The change in the relative population of the group II lines is a detail we have not clarified. The calculated rates of formation are not sufficiently accurate to determine if the change reflects the change in the $N_2(A)$ vibrational distribution or if another factor is involved. Figs. (13) to (15) suggest that group II does increase relative to group I as a result of the change in the vibrational distribution of $N_2(A)$.

The Quenching Step

In order to evaluate the importance of the quenching step, equation (5), relative intensities of long-lived states, the states expected to be most readily affected by the quenching reaction, were analyzed at different pressures. The radiative lifetimes of a number of the excited states were calculated according to the relationship

$$\tau^{-1} = g_j^{-1} \sum_i g_i A_{ji} \qquad (10)$$

and are summarized in Table VI. The g-values and gA values were taken from Moore[23] and Corliss and Bozman[24], respectively. Steady-state analysis of the mechanism, equation (5), gives

$$I_{rel}(Ni^*)^{-1} = \tau^{-1}/R + k_Q[N_2]/R \qquad (11)$$

where R is the rate of formation of Ni^*, and $I_{rel}(Ni^*) \propto [Ni^*]$. A plot of $I_{rel}(Ni^*)^{-1}$ against pressure will have a slope to intercept ratio of $k_Q\tau$. k_Q can be evaluated using the calculated values of τ.

The 3371.99A line originating from the long-lived 30980 cm^{-1} state is the one observed line which is drastically affected by pressure. This line, which is labeled in Fig. (4) through Fig. (11), drops in relative population by a significant degree between 0.13 and 27 torr. A graph of the reciprocal relative intensity, $I(3371.99)^{-1}$, against pressure is shown in Fig. (16). A value of $k_Q = 3\times10^{-10}$ is calculated using $\tau = 2\times10^{-8}$ sec. The data is very scattered but the quenching mechanism appears at least approximately correct. The calculated quenching coefficient is quite high, being essentially gas kinetic, i.e., the quenching reaction occurs on every gas kinetic collision. None of the lines originating from the other long-lived states showed any significant change. Lines originating from the 29833 cm^{-1} state, $\tau = 6\times10^{-9}$ sec, did not exhibit a change in relative population. The 2994.46A line, see Figs. (4) to (11), which originates from the 33590 cm^{-1} state, $\tau = 5\times10^{-9}$ sec, did exhibit a slight drop in relative population. It can be seen from Table VI that both the 30980 cm^{-1} and 33590 cm^{-1} states, in addition to having longer lifetimes, have nearby lower energy states within 100 cm^{-1} while the next lowest energy level below the 29833 cm^{-1} state is 400 cm^{-1} away. (At room temperature $kT \cong 200$ cm^{-1}). It appears, meager though the evidence is, that both a long radiative lifetime and a nearby acceptor state are necessary for the quenching step to be important. Ni^* is quenched to its next lower electronic state and N_2 absorbs the energy as an increase in translational energy. States with radiative lifetimes shorter than 5×10^{-9} sec were not affected by the quenching step.

ACKNOWLEDGEMENTS

We wish to thank Frank Kopak for performing the trap analysis and assisting with experiments while on an undergraduate NSF summer traineeship and Richard Gutowski for the standard lamp calibration of the monochromator and photomultiplier tube.

We also wish to acknowledge the support derived from using the facilities of the Laboratory for Research on the Structure of Matter, funded by the Advanced Research Projects Agency under contract DAHC15-67-0215 with the University of Pennsylvania.

REFERENCES

1. R. J. Strutt, Proc. Roy. Soc., A85, 219 (1911).
2. L. F. Phillips, Can. J. Chem., 41, 732 (1963).
3. L. F. Phillips, Ibid., 2060 (1963).
4. R. E. March and H. I. Schiff, Can. J. Chem., 45, 1891 (1967).
5. W. R. Brennen and G. B. Kistiakowsky, J. Chem. Phys., 44, 2695 (1966).
6. F. C. Fehsenfeld, K. M. Evenson, and H. P. Broida, Rev. Sci. Instrum., 36, 294 (1965).
7. W. R. Brennen and R. L. Brown, Rev. Sci. Instrum., 39, 608 (1969).
8. W. R. Brennen and E. C. Shane, J. Phys. Chem., 75, 1552 (1971).
9. R. R. Reeves, G. G. Mannella, and P. Harteck, J. Chem. Phys., 32, 946 (1960); G. G. Mannella, R. R. Reeves, and P. Harteck, ibid., 33, 636 (1960); P. Harteck, R. R. Reeves, and G. G. Mannella, Can. J. Chem., 38, 1648 (1960).
10. C. H. Corliss, J. Res. Nat. Bur. Std., 69A, 87 (1965).
11. A. I. Vogel, A Textbook of Quantitative Inorganic Analysis, John Wiley and Sons, Inc., New York, p. 415,479 (1966).
12. K. D. Bayes, Can. J. Chem., 39, 1074 (1961).
13. R. L. Brown and H. F. Broida, J. Chem. Phys., 41, 2053 (1964).
14. H. E. Radford and H. P. Broida, J. Chem. Phys., 38, 644 (1963).
15. I. M. Campbell and B. A. Thrush, Proc. Chem. Soc., 410 (1964).
16. D. W. Setser and B. A. Thrush, Proc. Roy. Soc. London A288, 256 (1965).
17. T. Iwai, M. I. Savadatti, and H. P. Broida, J. Chem. Phys., 47, 3861 (1967).
18. W. F. Meggers, C. H. Corliss, and B. F. Scribner, NBS Monograph 32, 1961.
19. W. W. Robertson, J. Chem. Phys., 44, 2456 (1966).
20. A. B. Callear and P. M. Wood, Trans Faraday Soc., 68, 272 (1971).
21. W. R. Brennen, R. V. Gutowski, and E. C. Shane, unpublished results.
22. W. Benesch, J. T. Vanderslice, S. G. Gilford, P. G. Wilkinson, Astrophys. J. 143, 236 (1966).
23. C. E. Moore, NBS Circular 467, vol. II, 1952.
24. C. H. Corliss and W. R. Bozman, NBS Monograph 53, 1962.

TABLE I: SUMMARY OF RELATIVE INTENSITIES

λ (Å)	E_u (cm^{-1})	Term Symbol	Relative Intensity (P) 0.13 torr.	(P) 0.31 torr.	(M) 0.4 torr.	(M) 1.1 torr.	(M) 2.3 torr.	(M) 9.6 torr.	(M) 14.7 torr.	(M) 27 torr.
2313.98	45419	w^3F_2	-	-	60	-	118	91	(44)	70
2325.79	44315	y^3G_4	-	-	63	-	-	-	-	-
2337.82	44475	w^3D_2	14	-	86	-	113	72	40	42
2337.49	42728	w^3D_3								
2424.03	42954	x^3D_2	19	-	72	-	73	34	16	18
53.99	42954	x^3D_2	(8)	-	30	-	-	10	-	-
72.06	42656	y^3P_1	18	-	55	-	31	25	-	-
76.87	40361	1_3^o	52	-	130	-	45	25	-	-
2981.65	34409	y^3D_1	105	115	90	145	85	250	330	520
94.46	33590	z^1G_4	1050	1100	950	920	700	570	560	580
3002.48	33501	y^3D_3	1550	1950	1700	2100	1900	3250	3900	5000
3.63	34163	y^3D_2								
12.00	36601	y^1D_2	660	950	740	1000	1100	1600	2300	3100
19.14	33112	y^3F_3	51	-	54	85	-	-	110	(56)
37.94	33112	y^3F_3	540	500	520	(650)	680	910	1000	1200
50.82	32973	y^3F_4	2250	2700	(1950)	2900	2600	2600	2700	2700

λ(Å)	E_u (cm^{-1})	Term Symbol	Relative Intensity (P) 0.13 torr.	(P) 0.31 torr.	(M) 0.4 torr.	(M) 1.1 torr.	(M) 2.3 torr.	(M) 9.6 torr.	(M) 14.7 torr.	(M) 27 torr.
54.31	33611	y^3F_2	480	420	360	670	710	900	1000	1300
57.64	34409	y^3D_1	-	520	470	770	780	1300	1700	2600
64.62	33501	y^3D_3	130	140	130	195	250	290	390	450
80.76	34163	y^3D_2	100	115	90	150	85	130	200	210
99.12	33590	z^1G_4	(125)	(240)	190	210	113	-	-	-
3101.56	33112	y^3F_3	2050	2500	2100	2900	2600	3100	3300	3600
3101.88	35639	y^1F_3	(40)	43	25	48	-	65	(70)	110
14.12	32982	z^1P_1	620	680	680	-	1100	1500	1900	1900
34.10	33611	y^3F_2								
3213.41	58526	e^5P_1	9	-	-	-	-	-	-	-
3214.06	56858	e^5D_4								
3215.82	57744	e^5D_3	16	-	-	-	-	-	-	-
3217.82	56821	e^5P_3								
3284.42	57104	i^3D_3	40	49	-	-	-	-	-	-
3369.57	29669	z^3D_3	500	500	500	500	500	500	500	500
3371.99	30980	z^3G_4	510	420	440	200	160	72±15	65±15	50±15
3374.22	29833	z^5F_3	-	-	(90)	(85)	59	-	(16)	-
74.64	56885	e^5H_7								
3380.57	32982	z^1P_1	680	630	590	560	670	690	790	1050
91.04	29481	z^3F_4	-	-	(130)	-	220	-	-	-
92.98	29669	z^3D_3	650	700	660	680	690	730	690	700
3414.76	29481	z^3F_4	1750	2000	1600	1700	1650	2100	1700	1800
23.71	30913	z^3D_1	340	320	340	350	380	280	250	260

λ(Å)	E_u (cm^{-1})	Term Symbol	Relative Intensity							
			(P) 0.13 torr.	(P) 0.31 torr.	(M) 0.4 torr.	(M) 1.1 torr.	(M) 2.3 torr.	(M) 9.6 torr.	(M) 14.7 torr.	(M) 27 torr.
3433.56	29321	z^3F_3	320	290	400	330	370	310	260	240
37.28	29084	z^5F_4	200	270	210	(170)	220	93	100	110
46.26	29888	z^3D_2	760	690	850	720	930	860	760	730
52.89	29833	z^5F_3	540	440	510	390	460	280	270	260
58.47	30619	z^3F_2	620	800	750	610	770	(650)	640	590
61.65	29084	z^5F_4	1450	1400	1500	1000	1400	(850)	800	720
67.50	30163	z^5F_2	85	-	(70)	-	-	-	-	-
72.54	30913	z^3D_1	320	300	330	280	400	280	330	370
83.87			120	140	140	110	113	85	100	110
92.96	29501	z^3P_1	600	530	700	500	900	(700)	690	730
3515.05	29321	z^3F_3	1100	800	1100	770	1350	850	680	(600)
24.54	28569	z^3P_2	1650	1500	2000	1250	2300	1850	1400	1400
66.37	31442	z^1D_2	680	580	880	(530)	1200	1200	1100	1250
71.87	29321	z^3F_3	100	110	130	80	110	85	-	-
87.93	28068	z^5G_4	180	100	120	(38)	-	-	-	-
3619.39	31031	z^1F_3	940	860	1200	800	1600	1200	860	880
3783.53	29833	z^5F_3	75	-	120	-	85	60	46	52
4401.54	48467	e^5F_5	330	350	430	270	380	300	200	150
35.35	52041	f^3F_2	38	-	58	29	25	(10)	-	-
4459.03	49086	e^5F_4	190	190	260	150	208	110	68	47
62.45	50346	e^5F_2	-	-	75	44	51	42	(28)	-
66.38	52272	g^3D_2	-	-	40	(25)	6	-	-	-

λ(Å)	E_u (cm^{-1})	Term Symbol	Relative Intensity (P) 0.13 torr	(P) 0.31 torr	(M) 0.4 torr	(M) 1.1 torr	(M) 2.3 torr	(M) 9.6 torr	(M) 14.7 torr	(M) 27 torr
4470.48	49778	e^5F_3	95	95	140	84	100	73	34	-
4600.36	50745	e^5F_1	32	-	70	37	-	24	-	-
5.00	49778	e^5F_3	74	100	-	85	125	64	44	35
48.65	49086	e^5F_4	135	185	300	150	85	100	85	49
86.21	50346	e^5F_2	(30)	-	-	34	26	(29)	22	23
4703.81	50754	f^1D_2	50	-	(80)	40	37	29	(22)	-
14.42	48467	e^5F_5	490	430	700	340	490	350	290	250
52.12	50706	e^1G_4	47	-	85	35	46	10	(13)	-
52.42	50537	e^1P_1								
56.51	40986	e^5F_4	100	140	200	93	145	64	47	35
63.93	50466	f^3F_4	40	-	90	39	-	21	(15)	(11)
86.54	48467	e^5F_5	145	180	220	115	171	125	105	83
4808.89	50678	e^3G_3	(58)	-	90	-	12	32	(19)	18
29.02	49271	f^3D_3	(160)	150	(260)	135	171	83	53	-
38.64	54251	g^3F_3	-	-	45	25	32	24	-	-
55.41	49159	e^3G_5	350	290	490	310	270	120	80	53
66.27	49086	e^5F_4	125	160	220	100	151	90	46	43
73.44	50346	e^5F_2	67	(90)	110	57	76	55	34	34
4904.41	48953	e^3S_1	280	250	430	180	240	120	65	46
13.97	51306	f^3F_3	54	-	80	40	47	32	(17)	26

λ(Å)	E_u(cm^{-1})	Term Symbol	Relative Intensity (P) 0.13 torr	(P) 0.31 torr	(M) 0.4 torr	(M) 1.1 torr	(M) 2.3 torr	(M) 9.6 torr	(M) 14.7 torr	(M) 27 torr
4918.36	51306	f^3F_3	100	155	230	110	148	95	63	46
4918.71	50717	f^3D_1								
4925.56	51306	f^3F_3	25	-	(30)	23	29	18	(10)	19
4935.83	52040	f^3F_2								
37.35	49333	e^3F_4	130	110	190	(93)	96	70	39	39
53.21	50346	e^5F_2	45	(60)	90	37	35	35	(28)	27
65.17	50754	f^1D_2	12	-	20	-	-	10	-	-
71.34	56711	f^3P_2	62	80	125	60	62	49	(31)	32
80.17	49158	e^3G_5	400	350	550	240	320	135	93	61
84.11	50678	e^3G_3	320	310	500	230	300	115	81	43
5003.74	33501	e^3F_3	135	170	230	100	108	48	(41)	26
17.58	48467	e^5F_5								
18.29	50834	e^3F_2	320	290	440	200	310	200	170	130
35.36	49175	e^3G_4	800	690	1100	530	690	250	180	130
35.96	49333	e^3F_4								
48.84	50832	e^1F_3	(100)	160	190	84	90	50	32	-
80.53	49158	e^3G_5								
81.11	50706	e^1G_4	1350	1400	2000	880	1000	470	320	220
84.09	49333	e^3F_4	470	(380)	(600)	320	410	-	(110)	86
99.31	49086	e^5F_4								
99.93	49271	f^3D_3	450	330	(500)	280	345	170	110	72

λ (Å)	E_u (cm^{-1})	Term Symbol	Relative Intensity							
			(P) 0.13 torr	(P) 0.31 torr	(M) 0.4 torr	(M) 1.1 torr	(M) 2.3 torr	(M) 9.6 torr	(M) 14.7 torr	(M) 27 torr
5115.39	50466	f^3F_4	280	260	(350)	200	250	120	87	48
25.23	49175	e^3G_4	(60)	-	110	56	60	27	(24)	(11)
29.37	49159	e^3G_5	90	(125)	160	77	66	44	(27)	28
42.78	49328	u^3D_3	280	210	320	170	160	-	63	53
46.48	49314	e^3F_3	320	340	500	240	290	140	78	68
55.12	50834	e^3F_2	240	220	340	180	180	-	53	76
55.76	50832	e^1F_3								
68.66	49175	e^3G_4	115	125	180	90	90	-	25	25
6176.81	49158	e^3G_5	-	-	-	-	60	41	-	-
7122.20	42606	e^3D_3	135	170	250	100	118	51	47	47
7393.60	42606	e^3D_3	21	-	75	38	-	20	16	11
7409.35	44112	e^3D_1	53	-	60	41	-	24	19	19
22.28	42790	e^3D_2	48	-	90	55	-	26	24	20
7555.60	44263	e^1D_2	-	-	85	-	-	32	24	21
74.05	44112	e^3D_1	-	-	(20)	-	-	12	(8)	-

Table II:

Summary of Reaction Conditions

Pressure	Discharge[a]	[N]	$[Ni(CO)_4]$	$\frac{[N]}{[Ni(CO)_4]}$
		$x10^3$, torr	$x10^3$, torr	
0.13	P	3.5	0.5	7.2
0.31	P	1.3	0.6	2.1
1.1	M	0.7	0.18	3.9
2.3	M	7.6	0.56	14
9.6	M	5.1	1.1	4.6
14.7	M	7.0	0.47	15
27	M	13	3.6	3.6

[a] P represents a pulsed discharge and M a Microwave discharge.

Table III:

Analysis of Solid Deposits

Source	Method[a]	%Ni
U-trap	EDTA	36
U-trap	EDTA	35
U-trap	DMG	70
inlet	EDTA	97
inlet	EDTA	95
inlet	DMG	92
inlet	DMG	94

[a]Titration with sodium ethylenediaminetetraacetate (EDTA) or precipitation with dimethylglyoxime(DMG).

Table IV:

CN Violet ($B^2\Sigma \rightarrow X^2\Sigma$) Relative Intensity

CN Band (v';v'')	Relative Intensity[a] 0.3 torr	0.4 torr	9.6 torr	14.7 torr	27 torr
3,2					320
2,1					270
1.0					210
4,4	(11)	(14)	210	140	490
3,3			155	95	320
1,1			137	85	310
0,0	32	21	210	140	510
5,7				28	95
0,1				28	42

[a]Inaccurately determined values are in parentheses.

Table V:

Relative Vibrational Population of $N_2(A^3\Sigma_u^+)$

$N_2(A^3\Sigma_u^+)$ v'	Relative Population 2.4torr	40torr
0	130	200
1	130	200
2	120	50
3	42	16
4	18	5

Table VI:

Calculated Radiative Lifetimes for Excited States of Nickel

E_u, cm^{-1}	τ X10^9, sec[a]	E_u, cm^{-1}	τ X10^9. sec[a]
28569	2.7	42790	1.3
29084	3.4	44112	(3.8)
29321	1.3	48467	0.34
29481	2.2	48953	2.3
29669	2.0	49086	0.23
29833	6.4	49158	0.37
29888	1.9	49159	0.88
30913	2.5	49175	0.41
30980	21	49271	1.3
31031	1.1	49314	(0.89)
31442	1.5	49328	(2.0)
32973	2.3	49333	(1.9)
32982	1.5	49778	0.37
33112	1.5	50346	0.33
33501	1.3	50466	0.70
33590	4.9	50717	0.51
33611	0.79	50832	(0.66)
34163	1.7	51306	1.3
34409	0.8	52040	(2.0)
35639	1.8		
36601	0.66		
42606	1.4		

[a]Calculated from $\tau^{-1} = g_u^{-1} \sum_{\ell} g_u A_{u\ell}$. For values in parenthesis g-values were not available.

FIGURES

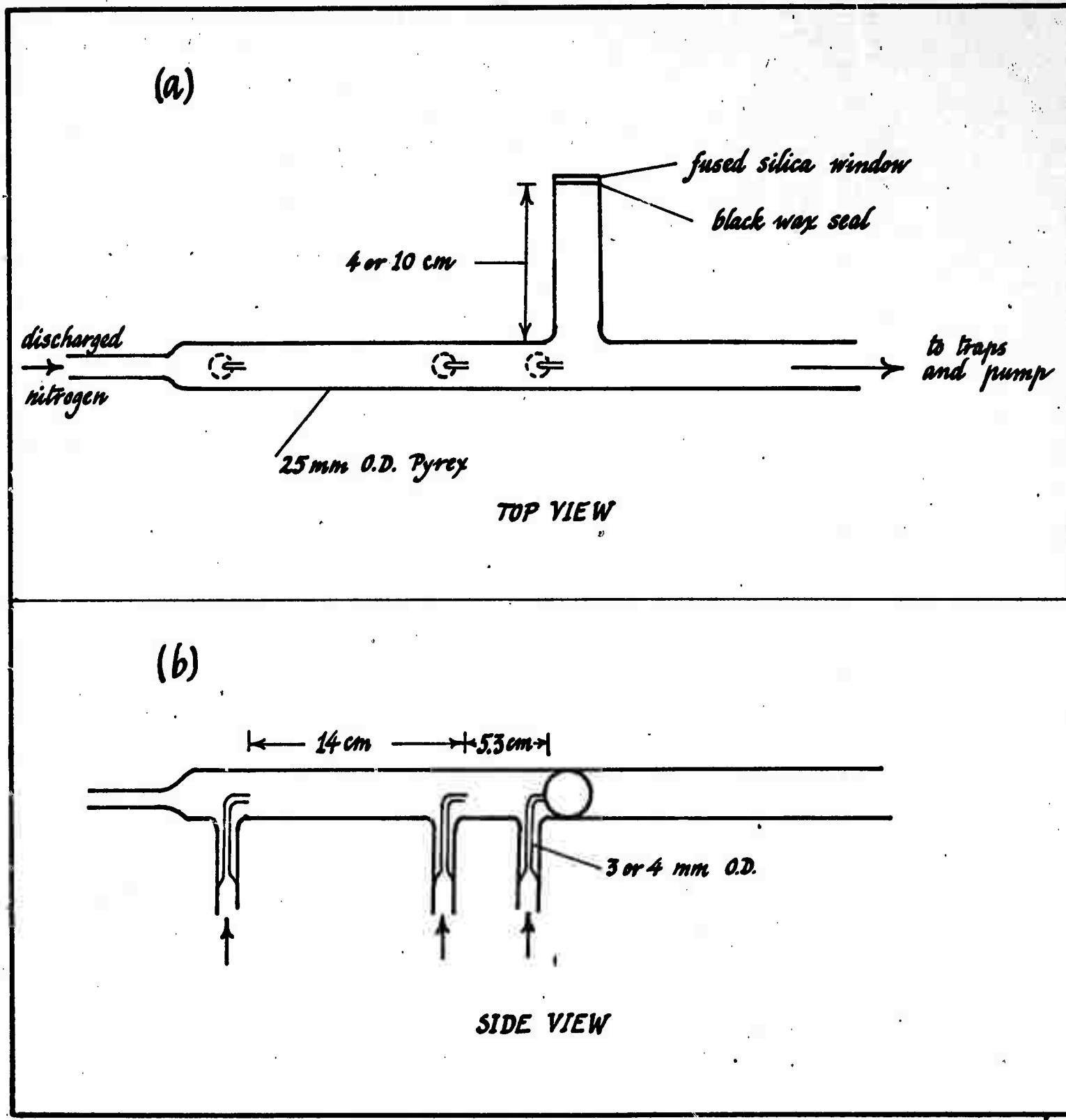
(a)
fused silica window
black wax seal
4 or 10 cm
discharged
nitrogen
to traps
and pump
25 mm O.D. Pyrex
TOP VIEW
(b)
14 cm
5.3 cm
3 or 4 mm O.D.
SIDE VIEW

FIGURE 1

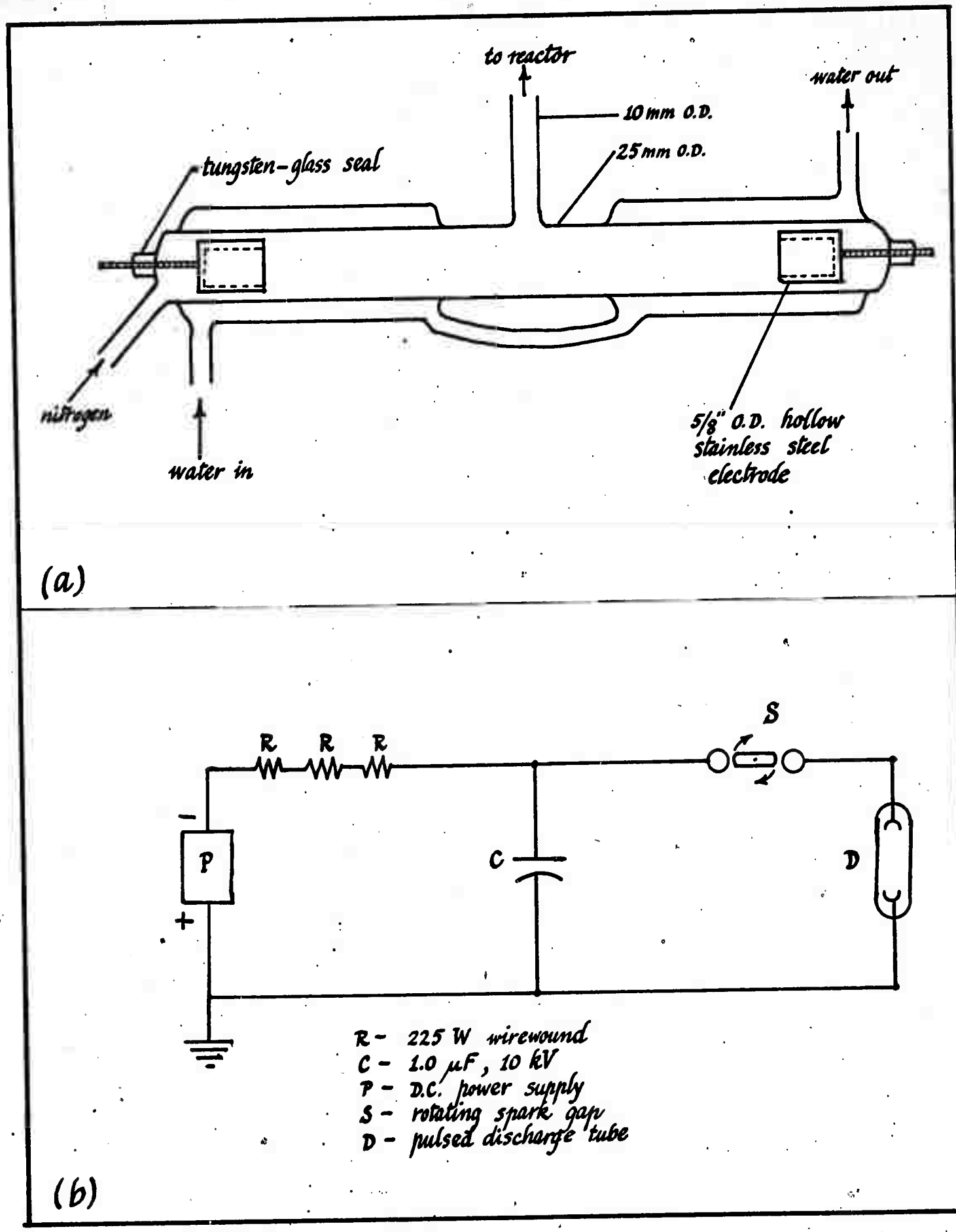
to reactor
water out
10 mm O.D.
25 mm O.D.
tungsten-glass seal
nitrogen
water in
5/8" O.D. hollow stainless steel electrode
(a)
S
R R R
P
C
D
R - 225 W wirewound
C - 1.0 μF, 10 kV
P - D.C. power supply
S - rotating spark gap
D - pulsed discharge tube
(b)

FIGURE 2

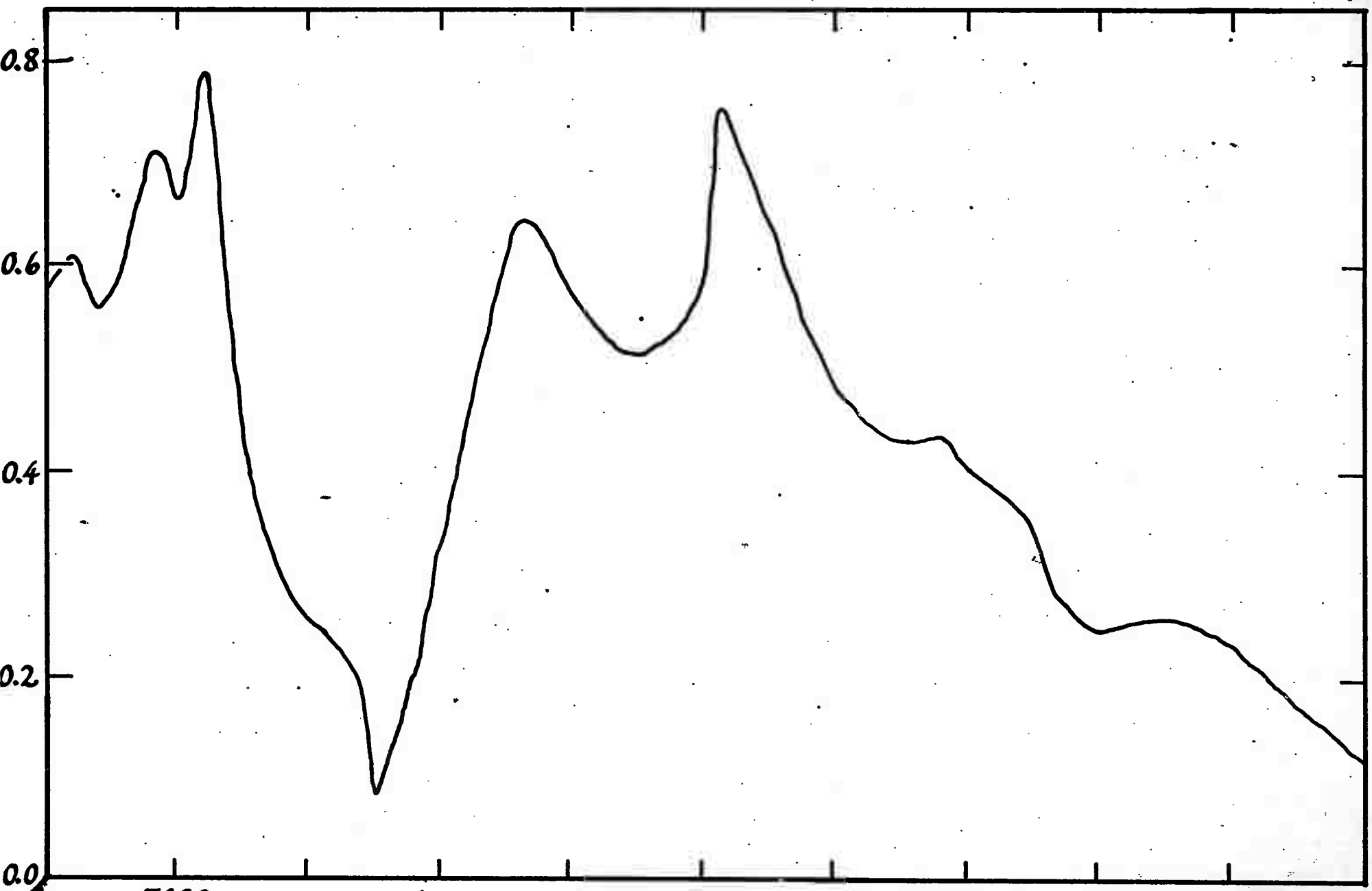

FIGURE 3

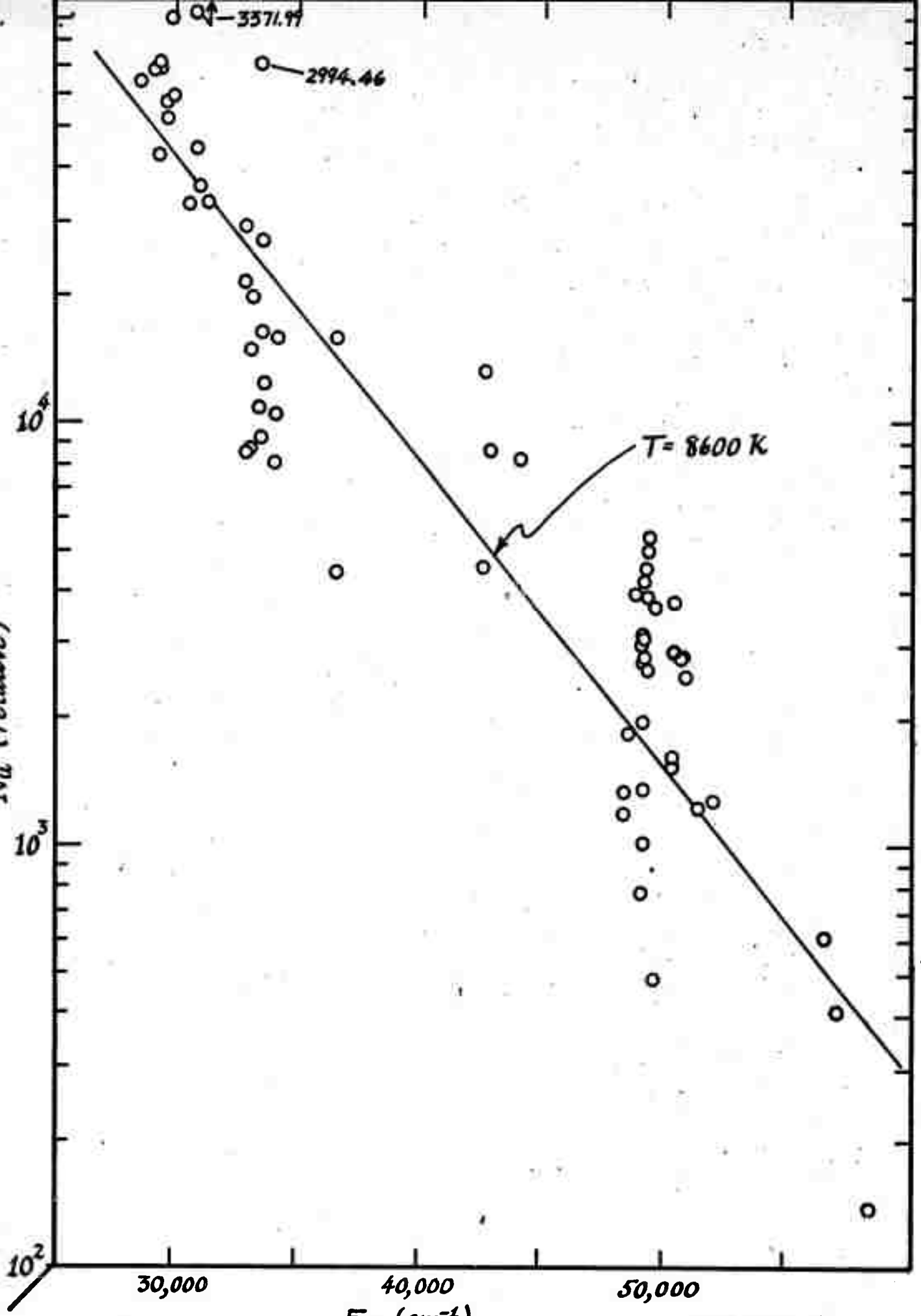
3371.91
2994.46
T= 8600 K
10^4
10^3
10^2
N_u (relative)
30,000
40,000
50,000
E_u (cm^{-1})

FIGURE 4

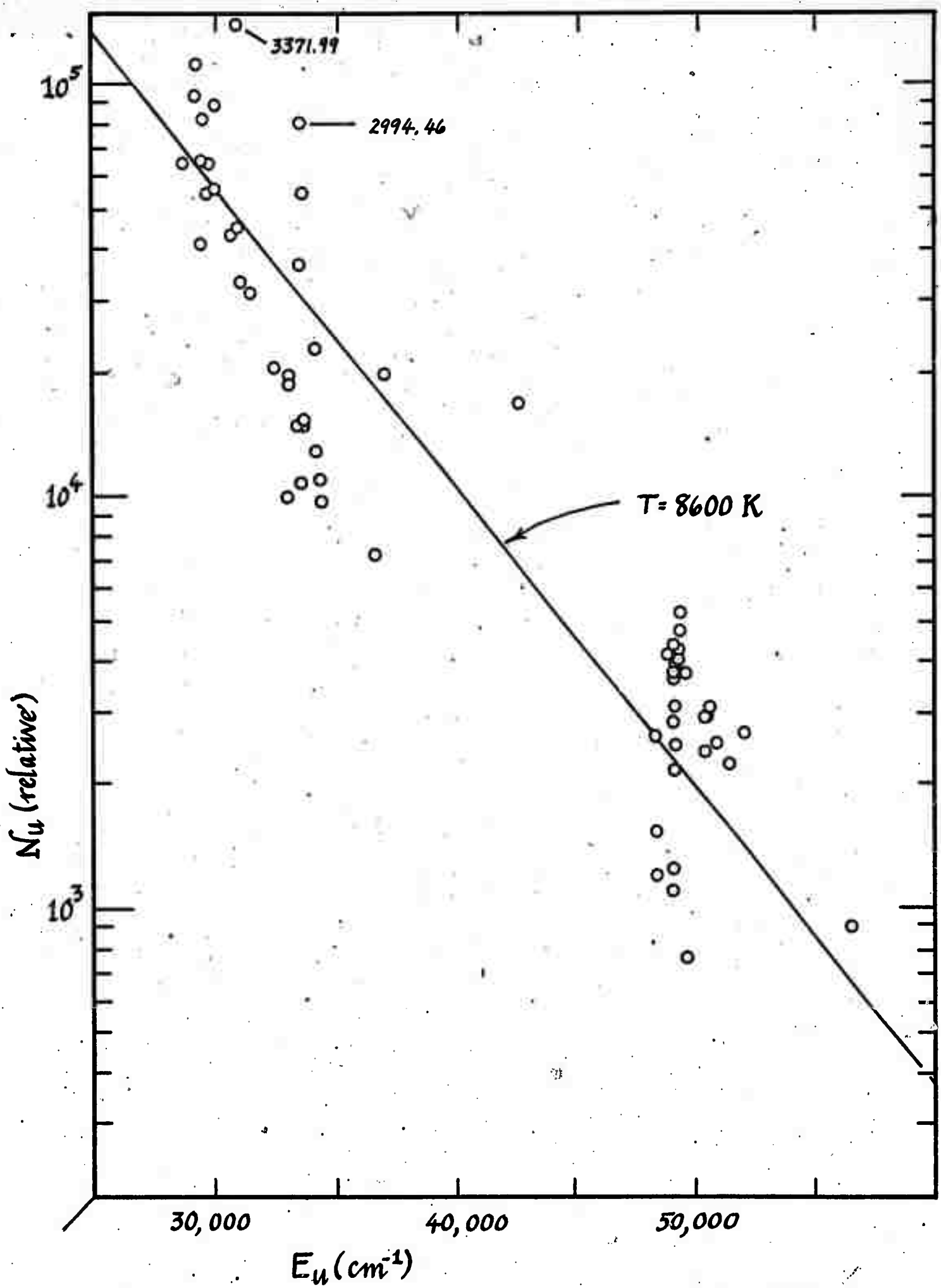
3371.99
2994.46
10^5
10^4
10^3
T = 8600 K
N_u (relative)
30,000
40,000
50,000
E_u (cm^{-1})

FIGURE 5

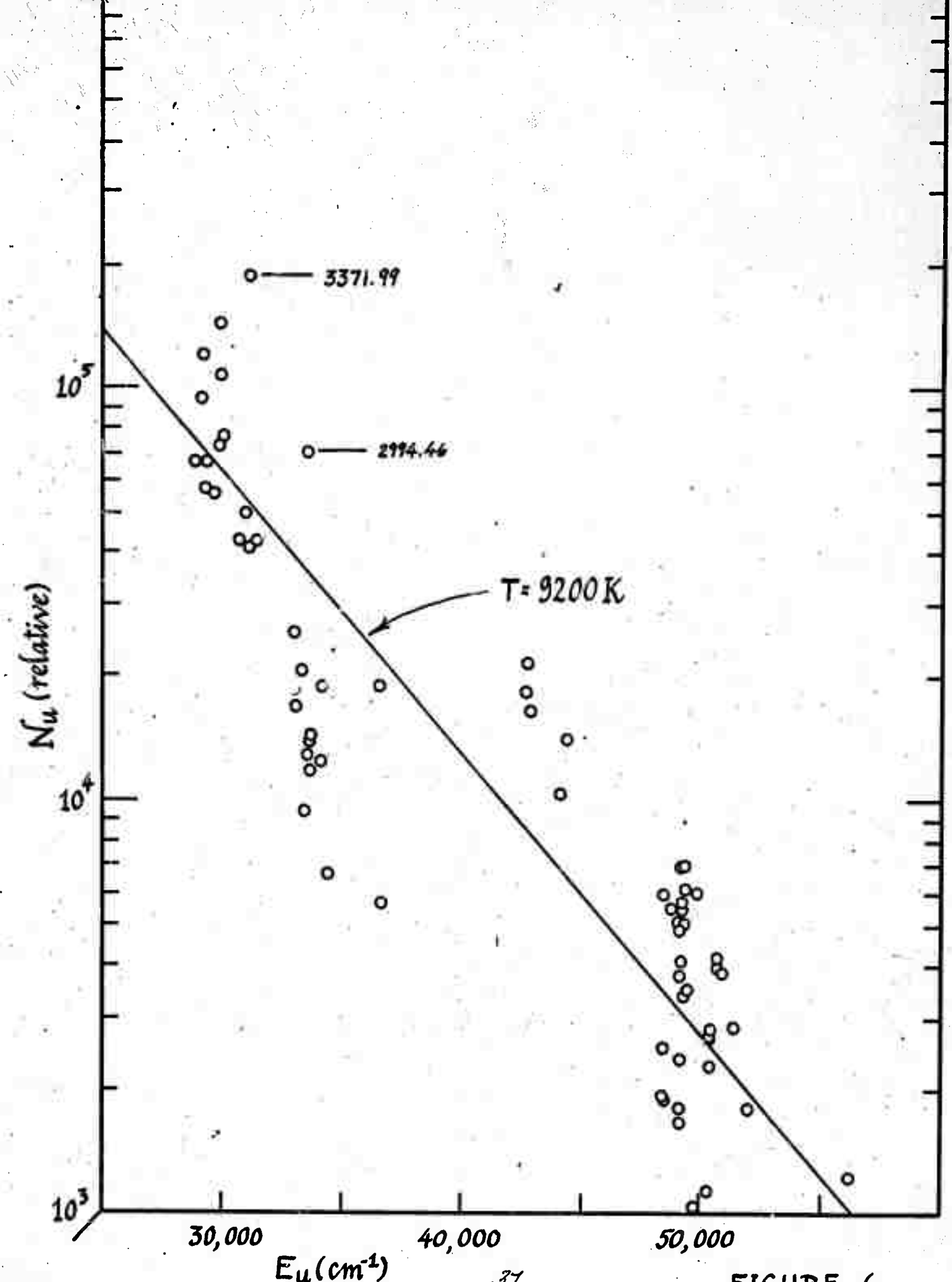
3371.99
2994.46
T = 9200 K
10^5
10^4
10^3
N_u (relative)
30,000
40,000
50,000
E_u (cm^{-1})

FIGURE 6

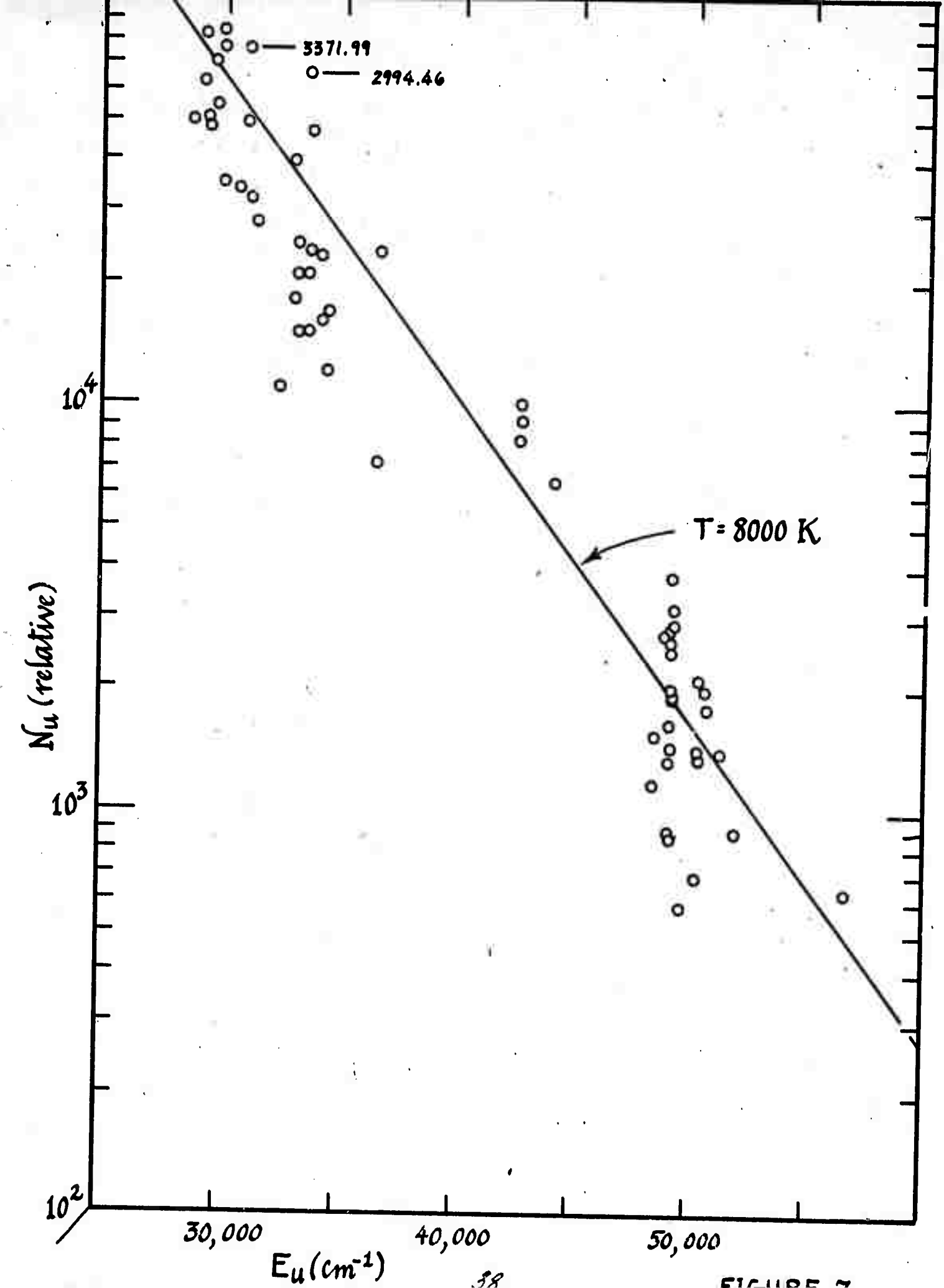
3371.99
2994.46
T = 8000 K
10^4
10^3
10^2
N_u (relative)
30,000
40,000
50,000
E_u (cm^{-1})

FIGURE 7

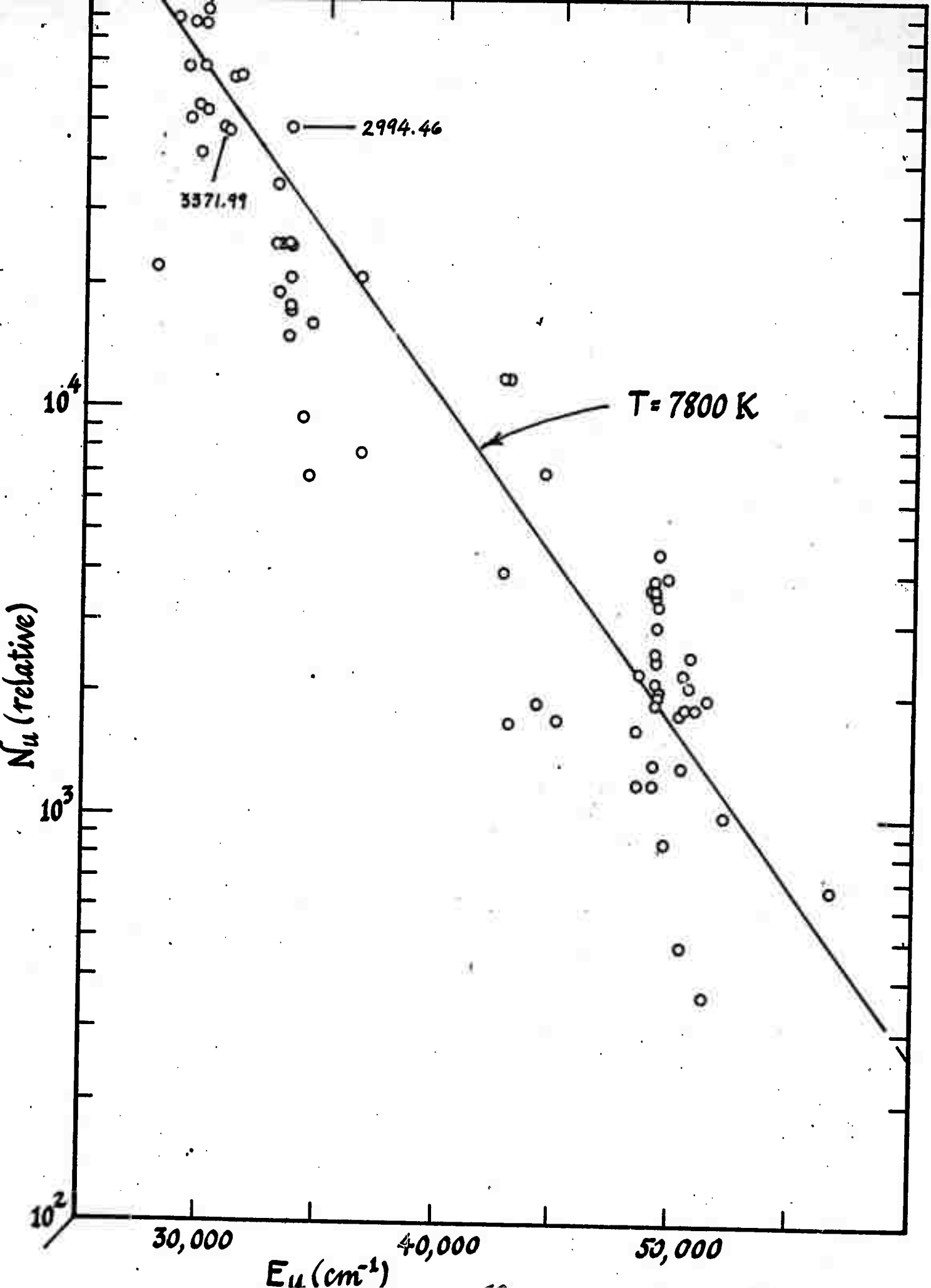
2994.46
3371.99
T = 7800 K
10^4
10^3
10^2
N_u (relative)
30,000
40,000
50,000
E_u (cm^{-1})

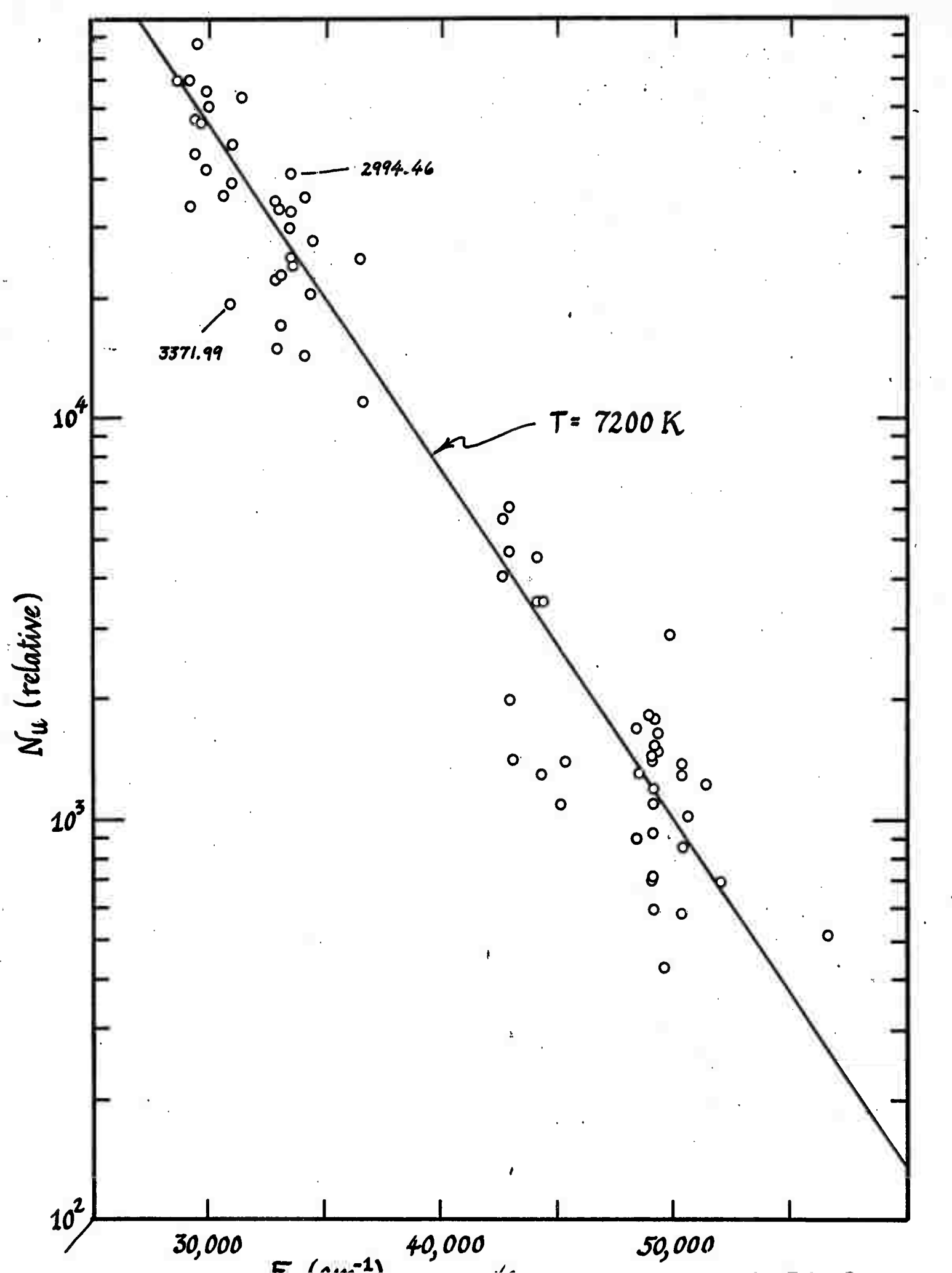
2994.46
3371.99
T = 7200 K
10^4
10^3
10^2
N_u (relative)
30,000
40,000
50,000
E (cm^{-1})

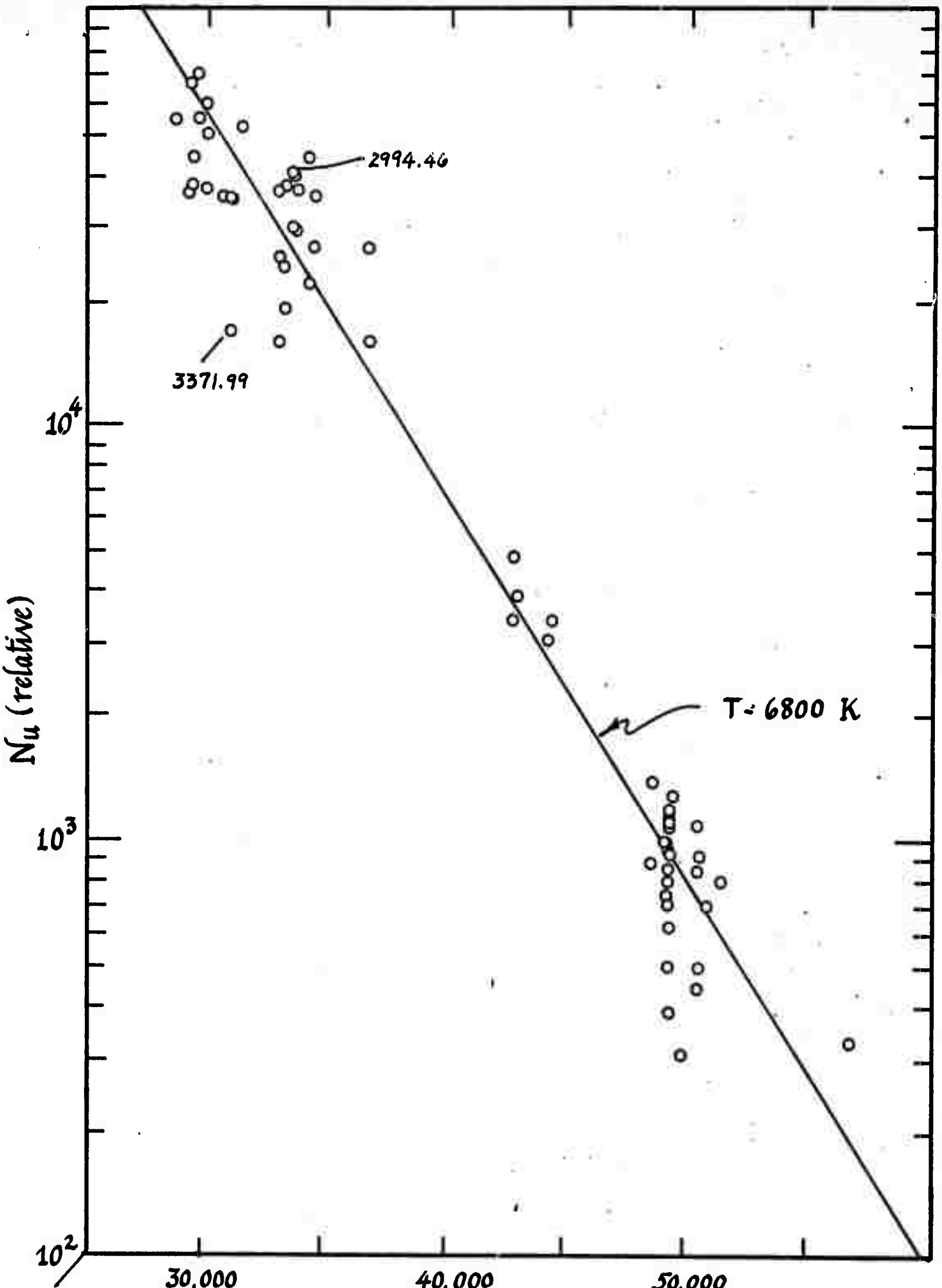
2994.46
3371.99
T = 6800 K
N_u (relative)
10^4
10^3
10^2
30,000
40,000
50,000

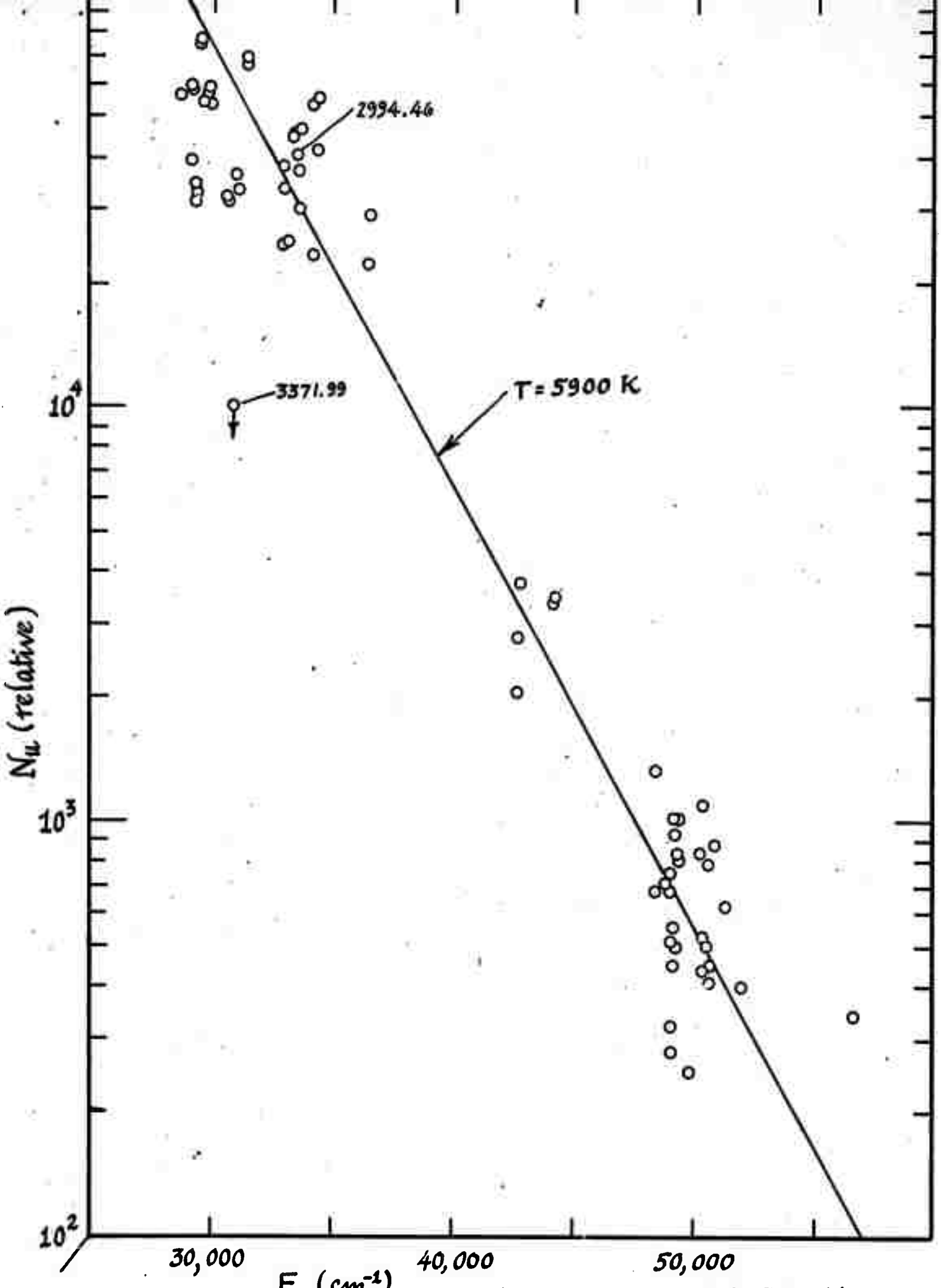
2994.46
3371.99
T = 5900 K
10^4
10^3
10^2
N_u (relative)
30,000
40,000
50,000
$E_u(cm^{-1})$

#2

FIGURE 11

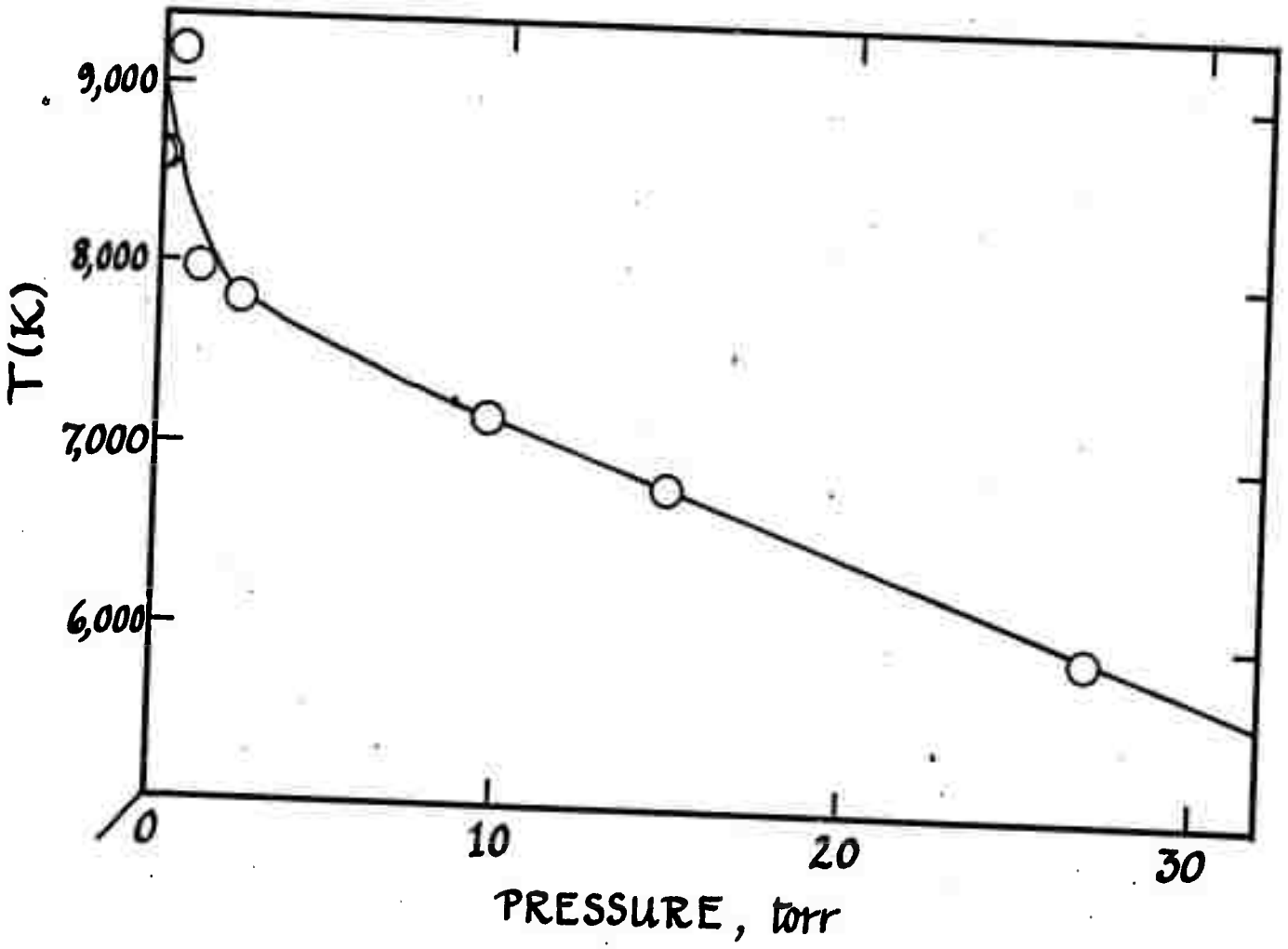

FIGURE 12

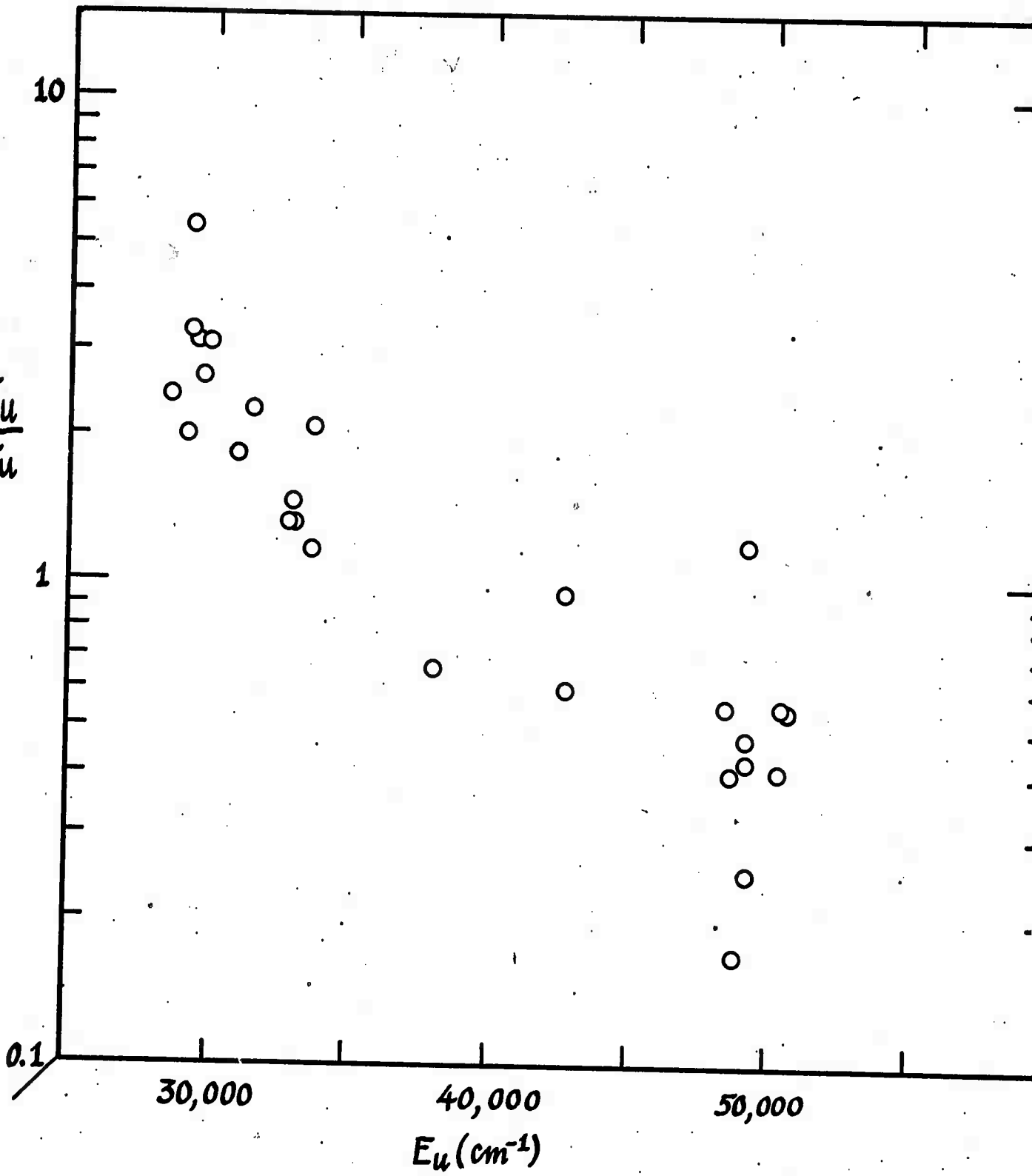

FIGURE 13

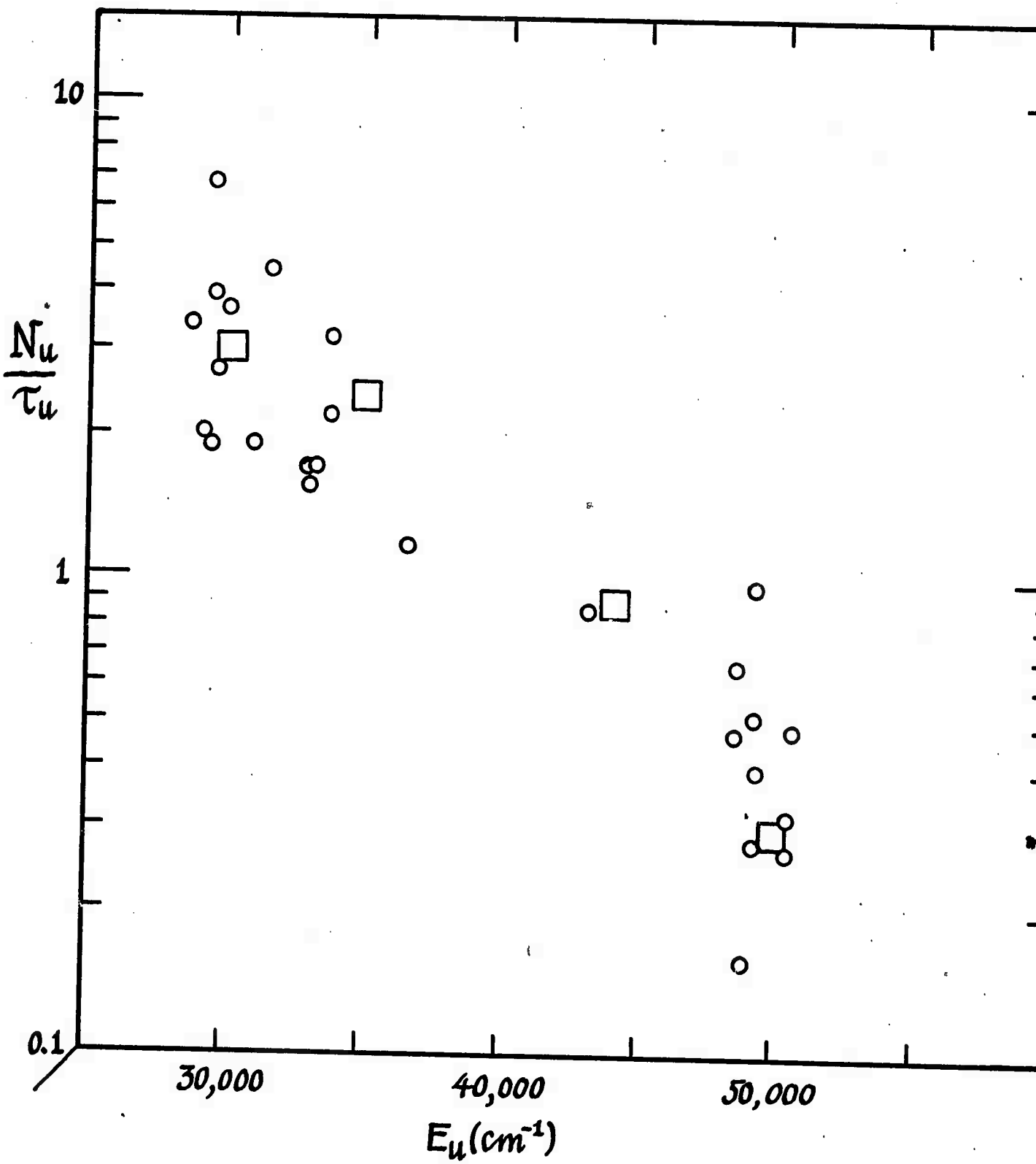

FIGURE 14

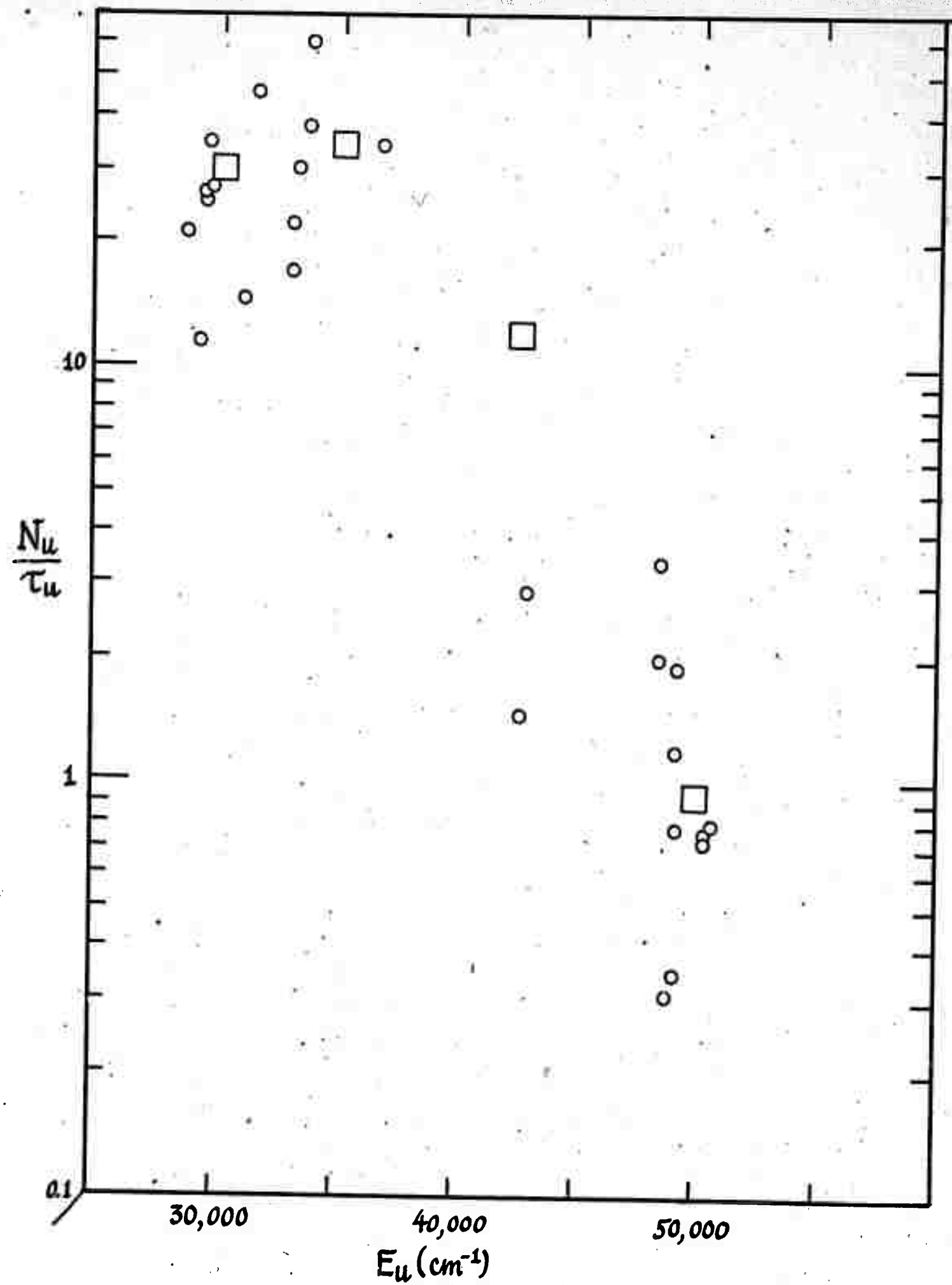
10
1
0.1
$\frac{N_u}{\tau_u}$
30,000
40,000
50,000
$E_u\,(cm^{-1})$

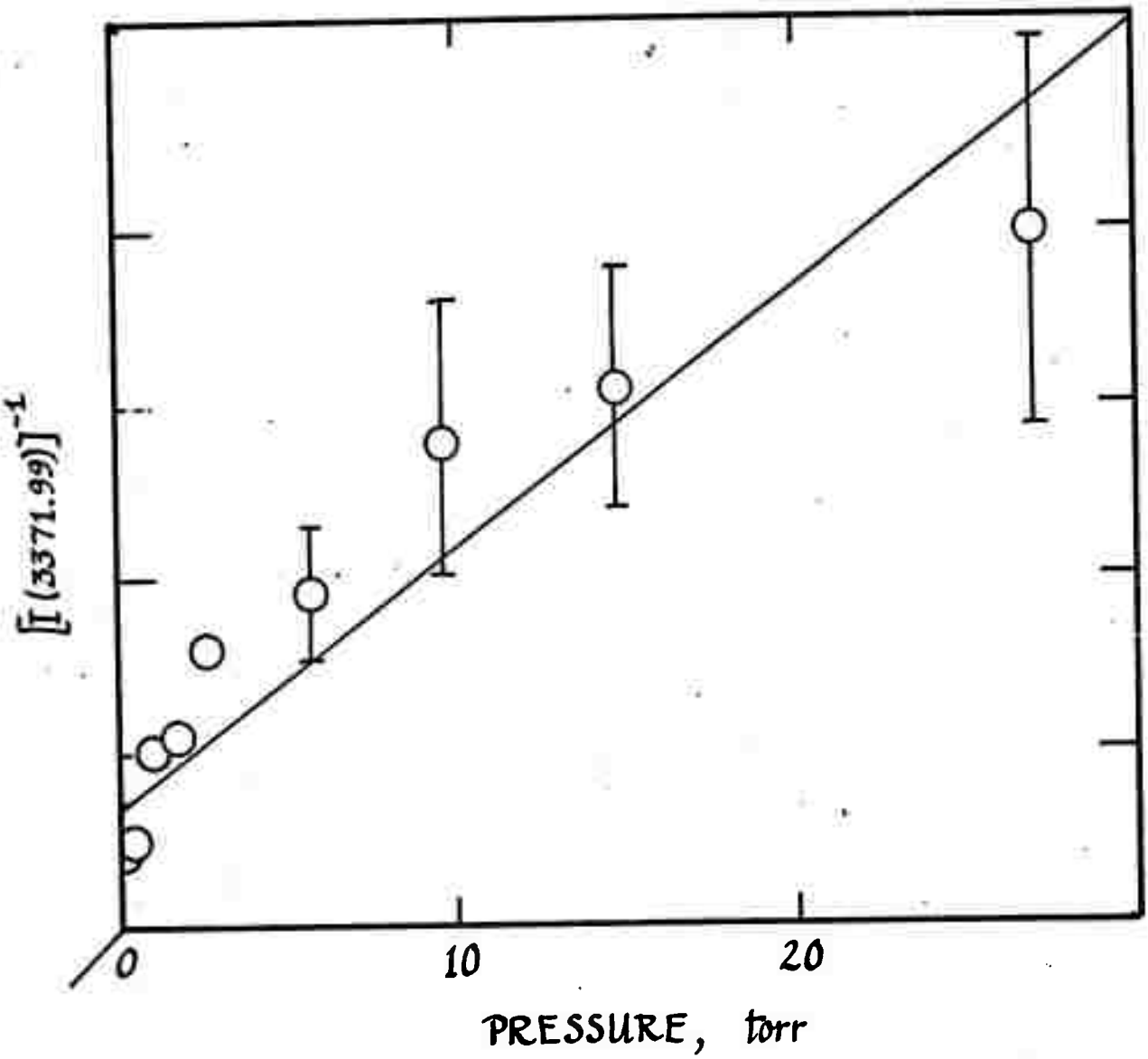

FIGURE 16